Chapter 4

Experimental Test Results

The purpose of this chapter is to present the experimental test results for the active control tests and the shunted PZT tests performed on the test plates. In addition, this chapter describes the development of the smart test plates, and the vibration characteristics of the test plates used in the experiments. The various test setups used to obtain the test results are also described.

4.1 Smart Test Plate Development

This section describes the development of the smart test plate used for the experiments run in the Advanced Vehicle Dynamics Laboratory (AVDL). Initial baseline tests were performed on the test plate and the frame to identify the plate's natural frequencies and resonant peak levels, which were later analyzed to determine mode shapes, or vibration patterns, of the test plate. This information was then used for optimum PZT placement and application. The test setups for the shunted PZT tests and the active control tests are also described.

4.1.1 Baseline Test Results

Baseline tests were performed on the undamped test plate to determine its vibration characteristics for the active and shunted PZT tests. The goal of establishing the vibration characteristics of the undamped test plates was to identify the modes that would be most successfully decreased using smart materials. In addition, the vibration characteristics provide information about the optimum placement of the PZT materials on the test plate

to maximize the overall control authority. For the shunted PZT tests, the modes were identified using a finite element model and laser-scanning techniques that measure velocity fields associated with the resonant frequencies.

4.1.1.1 Test Plate Resonant Frequencies

Baseline tests were performed on the undamped test plate in the shunted PZT and active control tests as described in Chapter 3. In these sets of tests, frequency response data was taken between the frame and plate from 0-400 Hz using the HP dynamic signal analyzer. The sampling technique, described in Section 3.2.3, used a uniform window, a span of 400 Hz, 800 spectral lines, an anti-aliasing filter, and 20 averages to collect the data. Figure 4.1 shows the results of a frequency response function taken in the shunted PZT baseline tests. This data was taken on an undamped plate that was later used for the shunted PZT tests, and similar to the plate used for the active control tests. The results show the resonant peaks of the undamped test plate, with the highest levels occurring at 43 Hz, 106 Hz, 145 Hz, and 252 Hz.

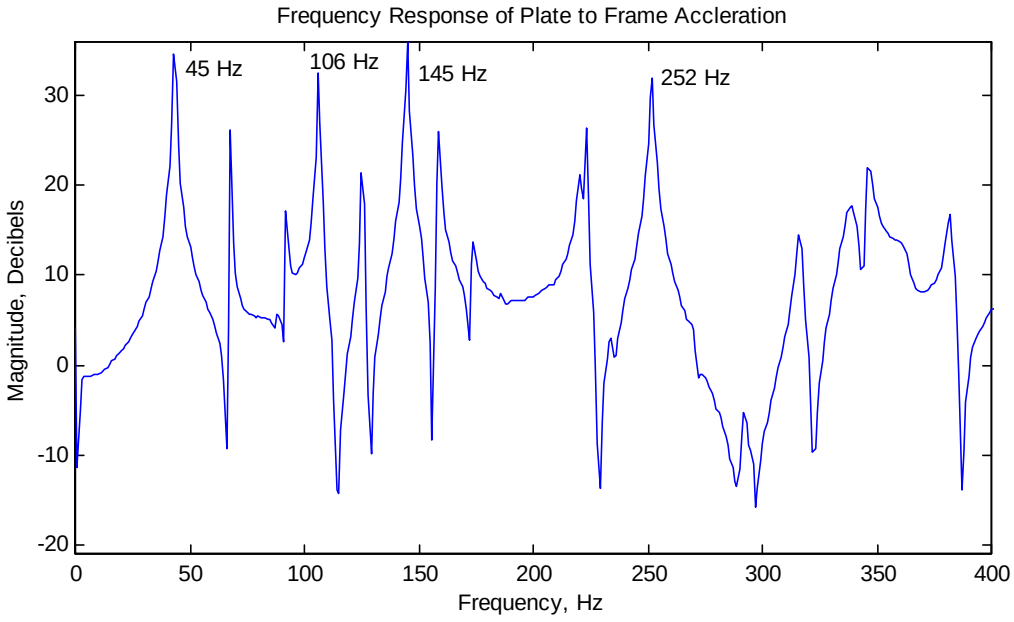

Figure 4.1. Baseline Test Results for Undamped Plate Used in Shunted PZT Tests [1]

For the active control tests, a new undamped test plate with the same overall dimensions and material as the test plate used for the shunted PZTs was used for the baseline tests. Figure 4.2 shows the frequency response results for the undamped test plate used in the active control tests. The results shown in Figure 4.2 differ slightly from those shown above in Figure 4.1 for reasons that could be a result of material defects, slight inconsistencies in material properties, or slight differences in dimensions. The small differences between the two plates, however, do not deter from using the new test data for our actively controlled PZT tests, nor do they prevent comparing the results for the shunted and actively controlled PZTs.

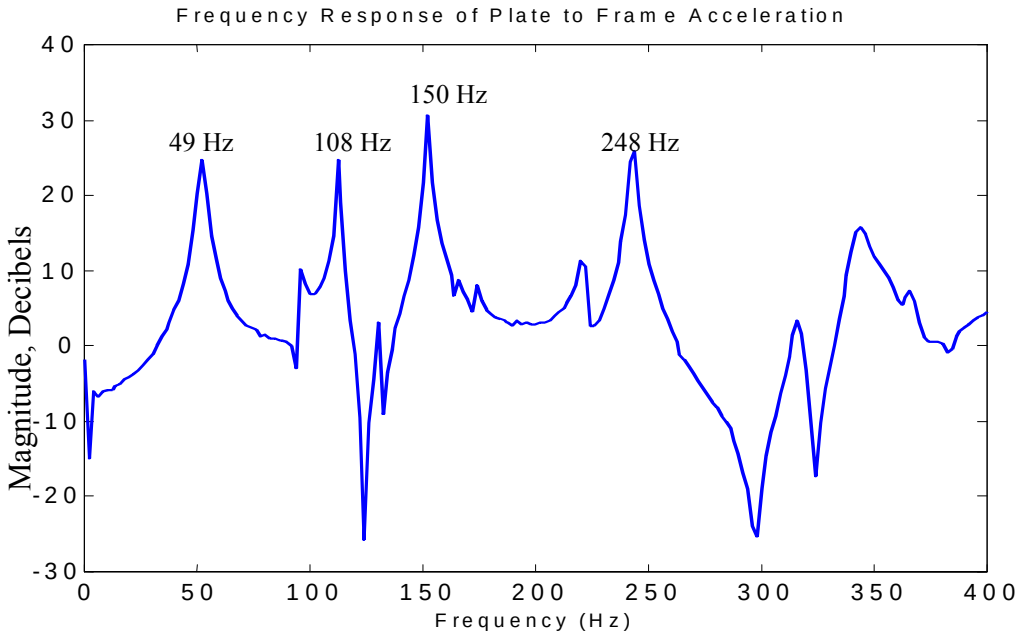

Figure 4.2. Baseline Test Results for Undamped Plate Used in Active PZT Tests

4.1.1.2 Test Plate Mode Shapes

The mode shapes for the test plate were determined analytically using Algor, a finite element package [27]. More specifically, this analytical analysis was performed using a 2000-element model of a plate with a 1.0 mm thickness, an area of 400 mm x 500 mm,

and fixed boundary conditions. The results of this finite element analysis can be seen in Figure 4.3. The numbers in parenthesis under each mode shape plot, (i,j), known as the mode index, are used to represent the number of half-sine waves along the width and length of the plate, respectively. For example, as shown in Figure 4.3, the (1,1) mode (one row and one column) at 44.2 Hz shows a bulge at the center of plate. Consistent with this convention, the (2,3) mode at 187.8 Hz shows two rows and three columns of bulges on the test plate. These results were used to determine PZT placement on the plate for maximum control authority. Kristina Jeric performed additional analyses, including laser-vibrometer testing on the plate [1]. It should be noted that the results in this analytical analysis are based on the assumption that the finite element package was able to find all modes in the frequency range of interest.

The resonant frequencies of the finite element model differ slightly from those obtained experimentally on the actual test plate. This could be a result of differences in boundary conditions, material properties, or dimensions between the finite element model and the actual test plate. The mode shape approximation, however, was deemed to be acceptable for the PZT placement and application for controlling the levels of vibration for the shunted and active PZT tests.

The application and placement of the smart damping materials was based on the mode shapes of the resonant frequencies in the frequency range of interest (0-400 Hz) and upon the experimental results. To achieve the greatest control authority of a mode, the actuator should be placed at a location with a high amount of strain energy for that particular resonant frequency. The active PZT tests show that a PZT actuator placed in the center of the test plate provides the greatest control authority of the modes from 0-400 Hz.

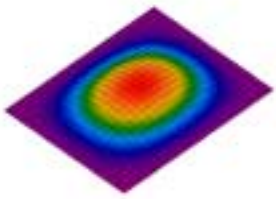

(1,1) Mode – 44.2 Hz

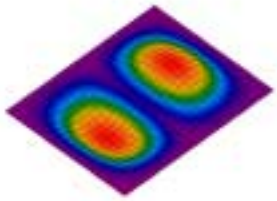

(1,2) Mode – 77.9 Hz

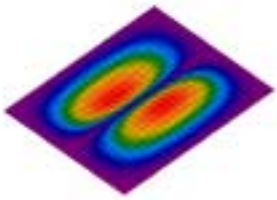

(2,1) Mode – 101.5 Hz

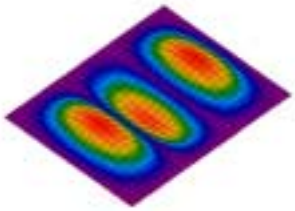

(1,3) Mode – 132.7 Hz

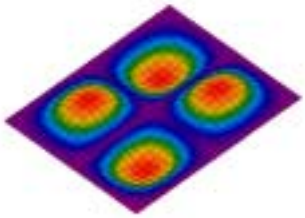

(2,2) Mode – 133.9 Hz

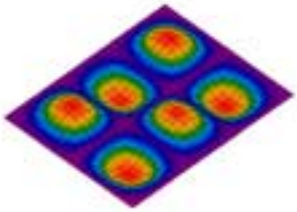

(2,3) Mode – 187.8 Hz

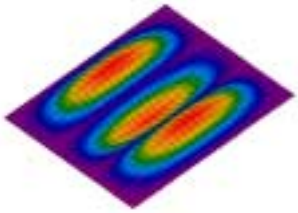

(3,1) Mode – 189.2 Hz

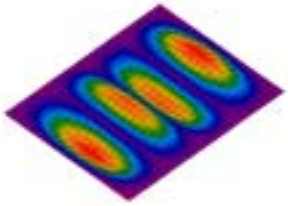

(1,4) Mode – 207.3 Hz

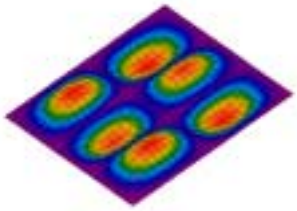

(3,2) Mode – 222 Hz

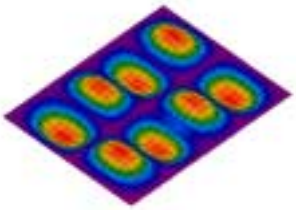

(2,4) Mode – 262.8 Hz

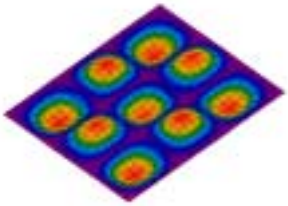

(3,3) Mode – 273.2 Hz

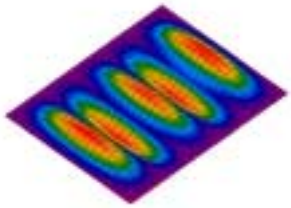

(1,5) Mode – 301.5 Hz

Figure 4.3. Finite Element Model Results for Test Plate

4.1.2 PZT Placement and Application

This section describes the PZT placement and application for the shunted PZT tests and the active control tests. The actuators used for both the shunted PZT and the active control tests were 2.85 in. square and 0.105 in. thick PZT patches bonded to the surface of the test plate. The smart materials used for testing are Model No. PSI-5H-S4-ENH PZTs and were obtained from Piezo Systems Inc. Additional information about the PZT materials can be found in Appendix D. For the passive control tests, three PZTs were applied to an undamped plate in the locations shown in Figure 4.4. These locations were chosen because they had high levels of strain energy for the resonant frequencies targeted for damping.

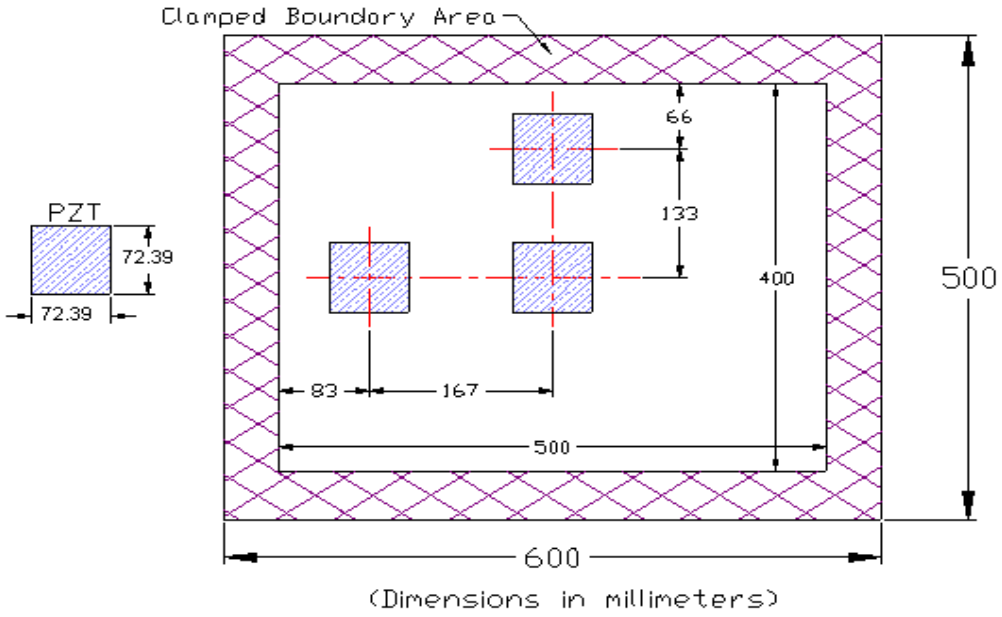

Figure 4.4. PZT Placement on the Test Plate for Shunted PZT Tests

The effect of the PZTs on the test plates was taken into consideration for both the shunted PZT tests and the active control tests. Figure 4.5 shows the effect of adding the three PZT actuators in the configuration shown in Figure 4.4. The results show that the

PZTs caused the frequency response peaks to shift to higher frequencies. In addition, the peak levels were decreased across most of the frequency range.

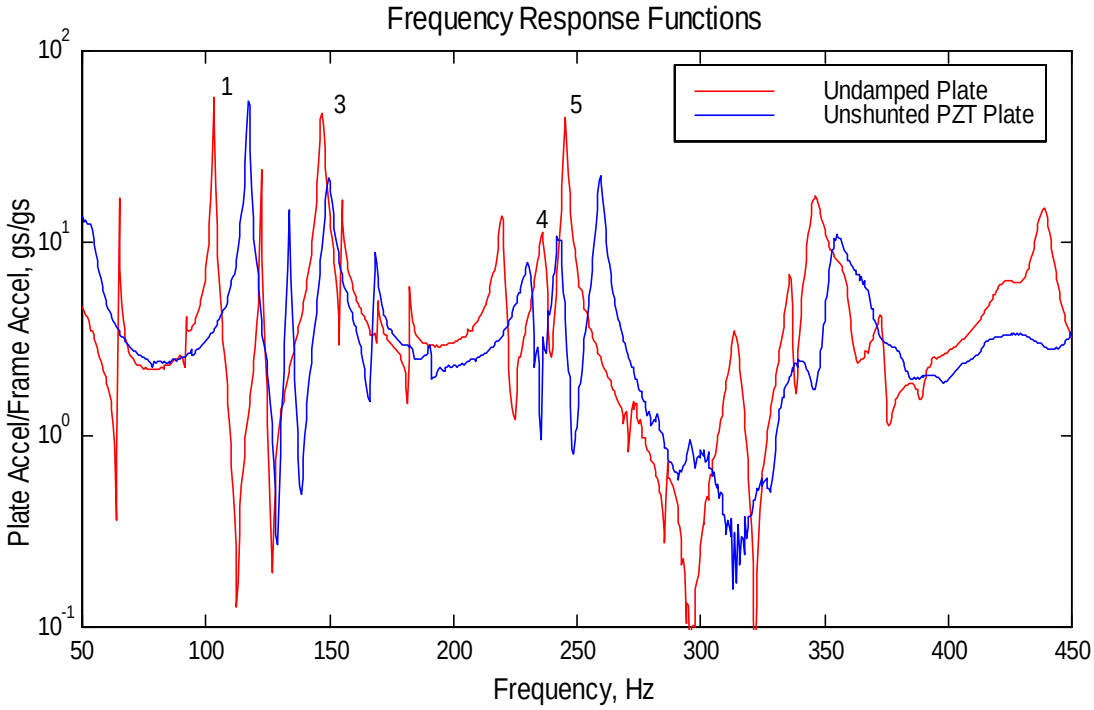

Figure 4.5. Effect of PZTs on Shunted PZT Test Plate [1]

The shunt circuit method of damping used in the shunted PZT tests did not have the same control authority as the active control techniques with positive position feedback. That is, the RLC shunt circuit method could be tuned to control one mode, or at most two closely spaced modes of the plate. Therefore, to successfully control the modes of the plate three actuators and three shunt circuits were needed. The active control method used only one actuator, the center PZT, to control multiple modes of the plate. Figure 4.6 shows the placement of the actuators on the active control test plate. Although there were two PZTs added to the actively controlled PZT plate, the center PZT had more control authority and was used as the actuator for controlling vibration levels.

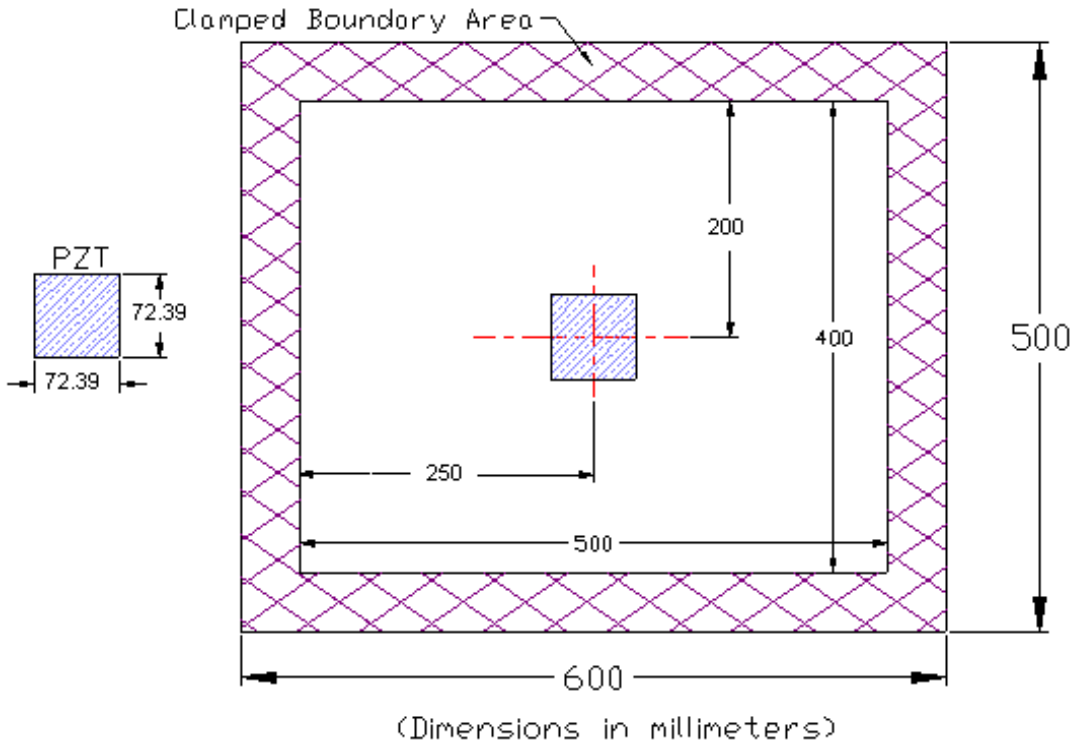

Figure 4.6. PZT Placement on the Test Plate for Active PZT Tests

The effect of adding PZTs to the surface of the active control test plate can be seen in Figure 4.7. The results in this figure show that the some of the more important peaks actually shifted to lower frequencies. Furthermore, the peak levels were decreased by the addition of the smart materials to the test plate. These frequency shifts and changes in peak levels can be attributed to structural effects of the PZTs on the test plate, such as increased bending stiffness and mass loading.

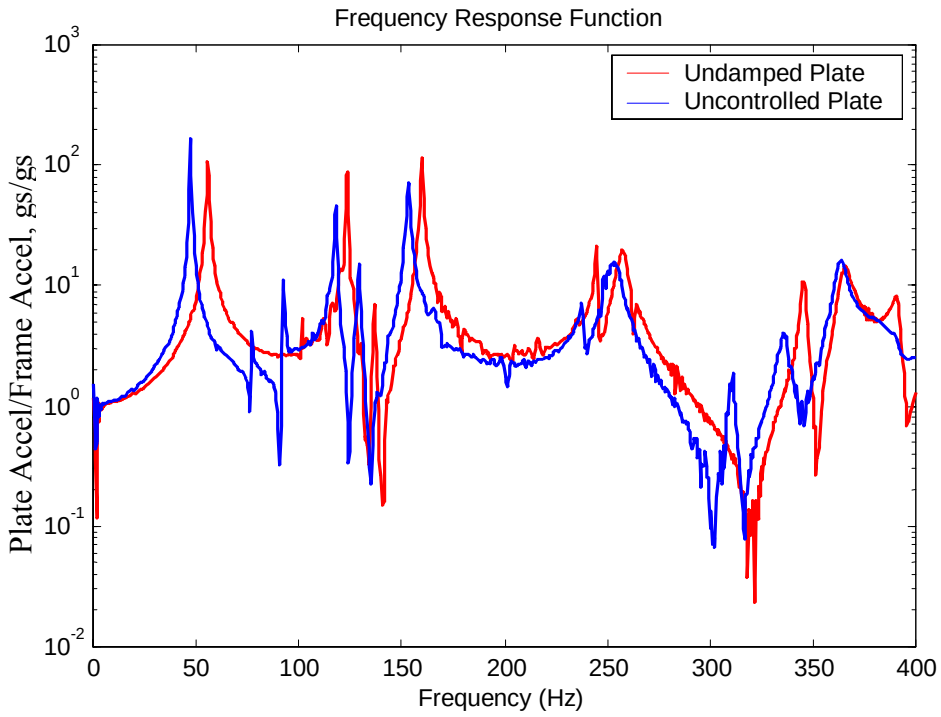

Figure 4.7. Effect of PZTs on Active PZT Test Plate

The method used to attach the smart materials to the test plates involved first sanding the surface where the PZTs are to be attached. This was done to make a better bond between the PZTs and the plate. The next step was to clean the surface of any dirt or metallic dust left over from sanding. Once the surface was cleaned, the PZTs were added to the plate using an adhesive called Loctite 94. A vacuum pump was then used as shown in Figure 4.8 to create a uniform distribution of the adhesive.

Figure 4.8. PZT Attachment with Vacuum Pump [1]

4.1.3 Smart Plate Test Setup for Shunted PZT Tests

In the shunted PZT tests, shunt circuits were used to dissipate energy from the modes they were targeted to control. There were three shunt circuits tuned to control different modes of the test plate. Each shunt circuit was tuned to a specific frequency using the design procedure discussed in Chapter 2, which involved calculating the initial resistor values and then making small adjustments to obtain the optimum amount of damping. The test setup used in the shunted PZT tests can be seen in Figure 4.9. The HP dynamic signal analyzer used for data acquisition and the power-supply used to power the operational amplifier of the shunt circuit are not shown in this figure. A block diagram showing the entire test setup for the shunted PZT tests can be seen in Figure 4.10. This figure shows the data acquisition system, the power supply, and the shunt circuits in relation to the overall test setup. A more detailed description of the test setup used for the shunted PZT tests can be found in Kristina Jeric's thesis. [1]

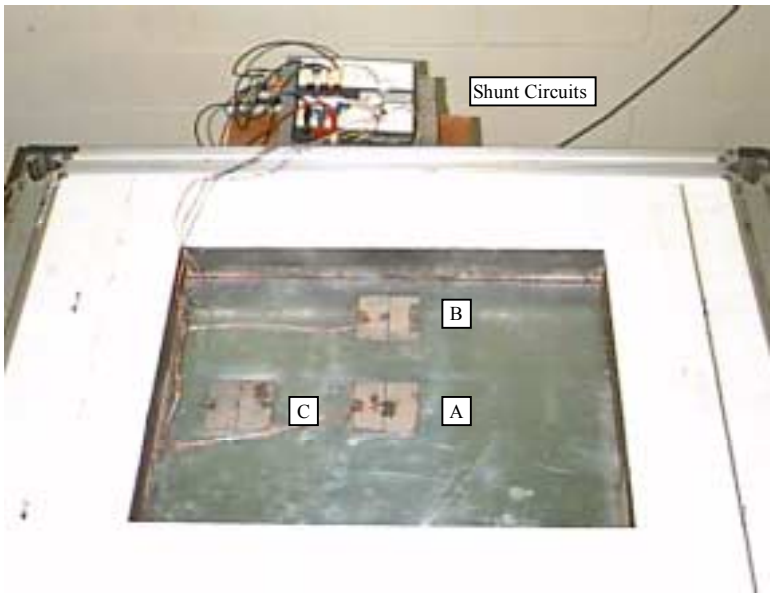

Figure 4.9. Smart Damping Plate Test Setup for Shunted PZT Tests [1]

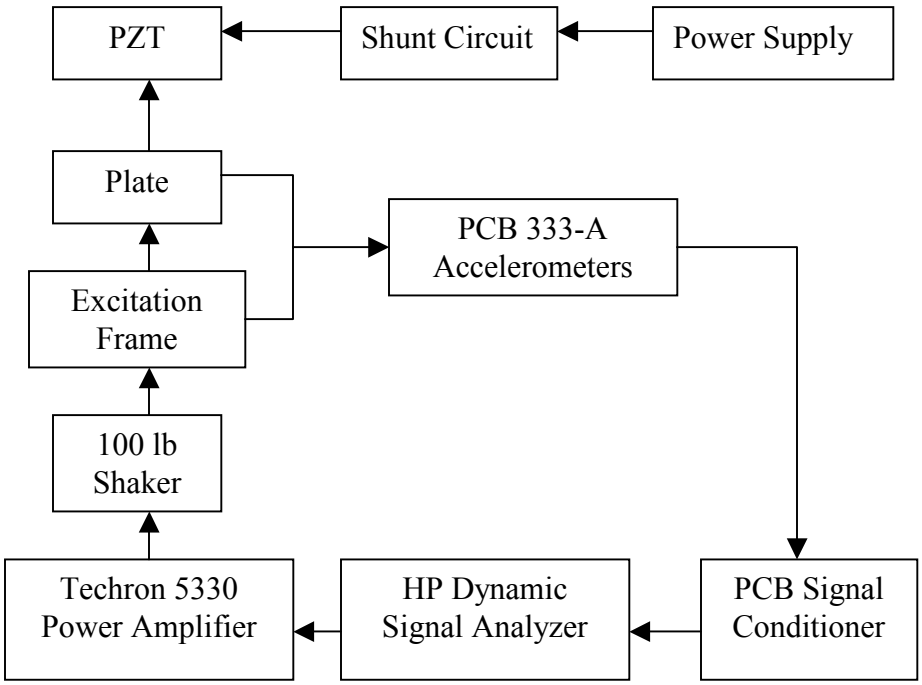

Figure 4.10. Overall Test Setup for Shunted PZT Tests

4.1.4 Smart Plate Test Setup for Active PZT Tests

The goal of the active control tests was to establish a technique for vibration suppression in a representative aircraft panel. This technique combined the technology of optical fiber sensors with piezoelectric actuators to minimize the vibration levels in the test article. The specific control law used for the active control tests is called Positive Position Feedback (PPF). This control law uses a generalized displacement measurement from the test article to accomplish the vibration suppression.

The test panel used for the active control tests is a 500 mm x 600 mm, 20-guage, galvanized steel plate with two 2.85 in. x 2.85 in. piezoelectric actuators bonded to its surface. The smart test plate setup for the active control tests can be seen in Figure 4.11. These two locations were chosen for the actuators because the test plate had a large amount of strain energy in these regions for the modes that needed to be controlled. In general, the control authority of an actuator is increased when it is placed in a region of high strain energy such as an anti-node of a mode. Although the test plate has two piezoelectric actuators attached to its surface, it was determined that the center PZT was

more effective at minimizing the levels of vibration. The center PZT was the only actuator used to minimize the vibration levels of the test plate.

Figure 4.11. Smart Test Plate for Active PZT Tests

The sensor used for the feedback control was a modal domain optical fiber sensor for vibration monitoring. This sensor is based upon a laser that focuses coherent light through a lens into one end of a multimode optical fiber [28]. One end of the fiber was attached to the plate and the other end of the optical fiber passed through a spatial filter and into a photodetector. The output of the photodetector is a variable voltage that is fed into a monitoring unit such as an oscilloscope. The optical fiber sensor used in the active control tests is an Extrinsic Fabrey-Pero Interferometer (EFPI) sensor. This sensor is illustrated in Figure 4.12.

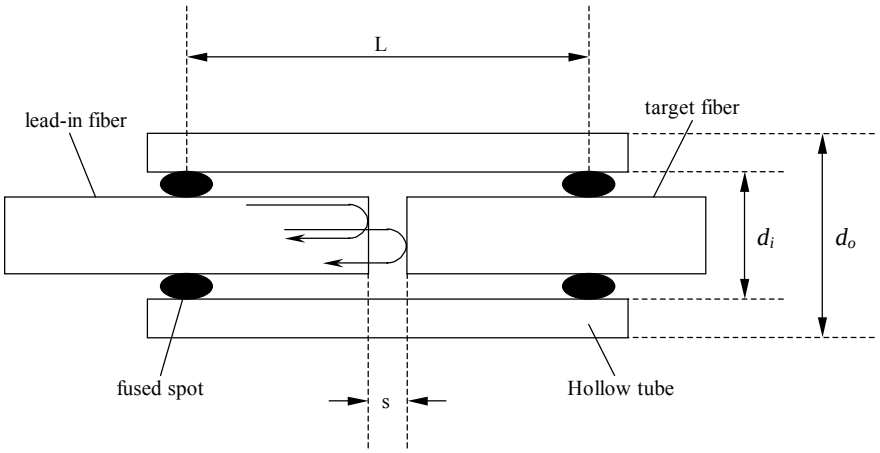

Figure 4.12. A Schematic Illustration of EFPI Fiber Optic Sensor

The system's parameters and the overall control system's performance were measured using a two channel HP Dynamic Signal Analyzer. This signal analyzer was used to get the frequency response function between the plate and the clamping frame using two accelerometers, one on the bottom center of the plate and one on the clamping frame, as described in Sections 3.2.2 and 3.2.3. A complete system block diagram showing the overall test setup for the active control tests can be seen in Figure 4.13.

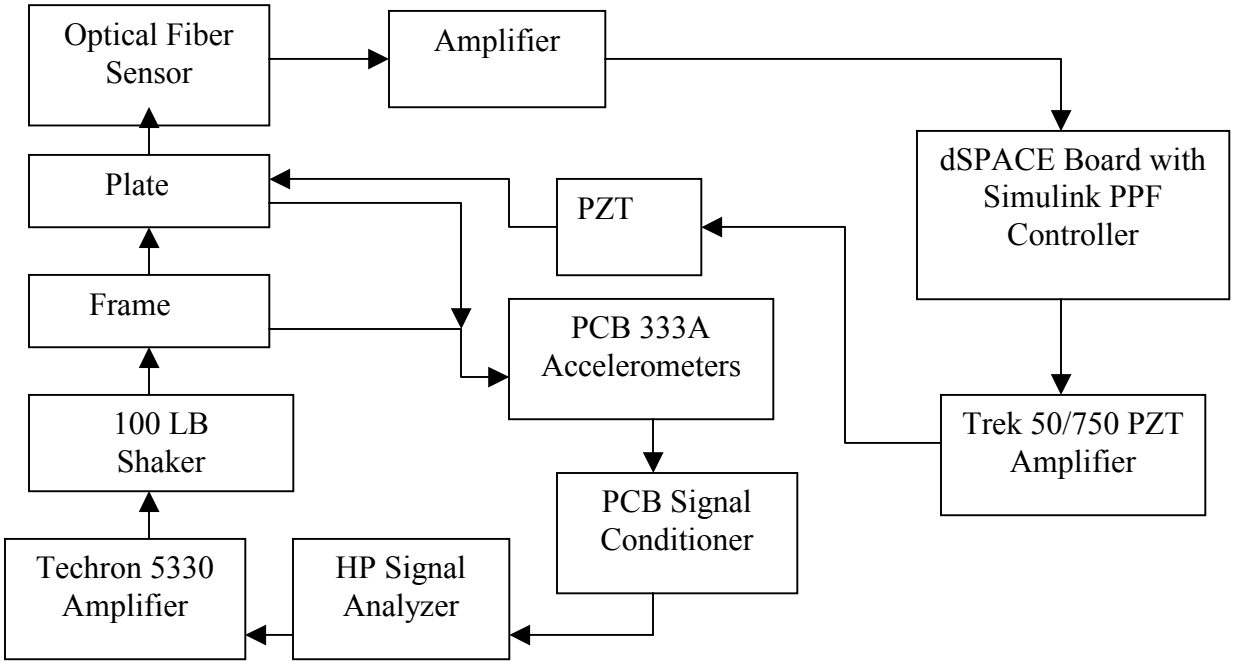

Figure 4.13. Active Control Test Setup

4.2 Shunted PZT Testing Procedure and Results

This section presents the testing procedure and the results obtained in the shunted PZT tests conducted on the test stand described in Chapter 3. These results are presented such that a direct comparison could be made with the results obtained in the active control tests. It should be noted that between the active control and shunted PZT tests, different frequency ranges were used to excite the test plate. For the shunted PZT tests, the frequency range was kept to 50-450 Hz because of the acoustic analysis and the specific limitations of the reception chamber. The reception chamber (Top Box) was designed for acoustic testing above 50 Hz; therefore, the frequency range for the shunted PZT tests was limited to frequencies above 50 Hz. At this time, the results for the shunted PZT tests are limited to the 50-450 Hz frequency range.

The goal of the shunted PZT tests was to obtain the maximum amount of damping using shunt circuits and piezoelectric materials. As previously explained, the PZTs were placed in areas of high strain energy to achieve the largest amount of vibration suppression. Several tests were conducted in the Advanced Vehicle Dynamics Laboratory to determine which PZTs would best damp-out which modes of the test plate. The results of these tests provided a shunting strategy that was used for the PZT shunt circuit tuning, which can be seen in Figure 4.14. This figure shows that the left PZT was best suited for damping the mode at 101 Hz, which is a one-three mode of the plate. In addition, the PZT located at the top of the plate was best suited for damping the mode at 147 Hz, which is a three-one mode of the plate. The center PZT was used to attack two modes of the plate: the mode at 235 Hz, and the mode at 245 Hz. For these two modes, the shunt circuit was tuned to a frequency between 235 Hz and 245 Hz. The three circuits used for the shunted PZT tests were tuned individually for the modes they were best suited to control.

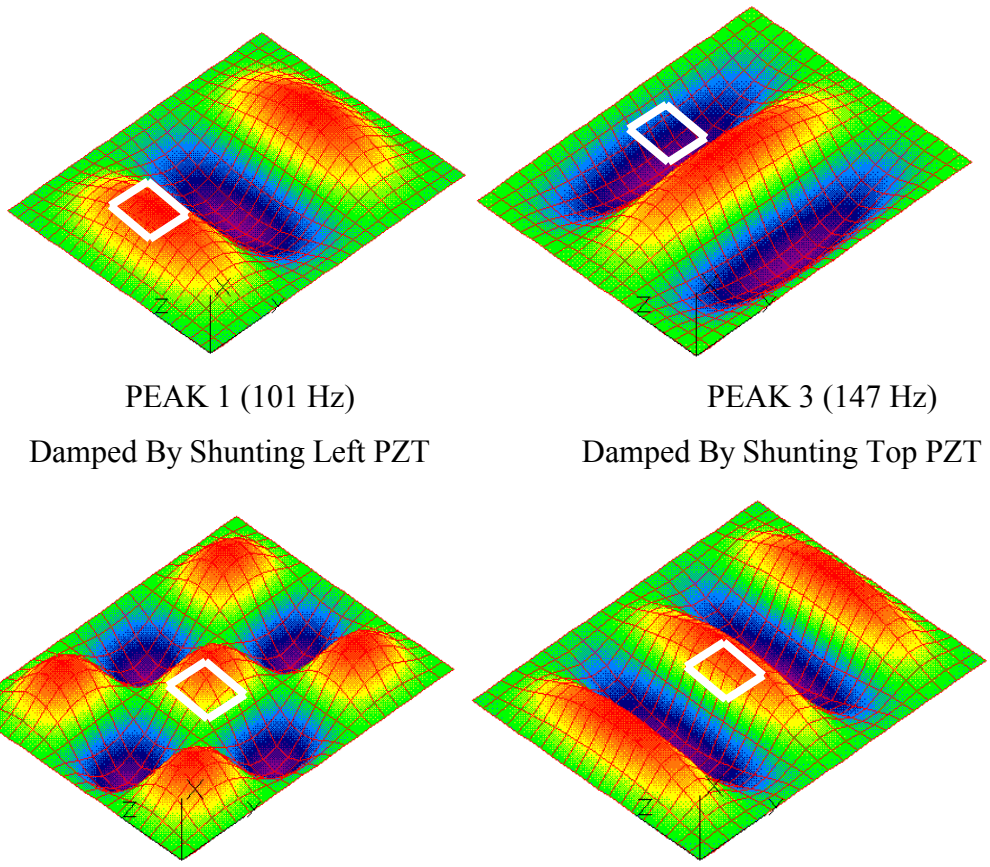

PEAK 1 (101 Hz)
Damped By Shunting Left PZT

PEAK 3 (147 Hz)
Damped By Shunting Top PZT

PEAK 4 (235 Hz)
Damped By Shunting Center PZT

PEAK 5 (245Hz)
Damped By Shunting Center PZT

Figure 4.14. PZT Placement and Shunting Strategy [1]

Once the shunting strategy was developed, initial tests were performed on the shunted and unshunted test plates. The objective of these tests was to tune the shunt circuits to the resonant frequencies of the plate between 50 and 450 Hz. The tuning procedure used for the shunt circuits is described in Chapter 2. Figure 4.15 shows the results of the frequency response tests conducted on the shunted and unshunted test plates. The results of this figure show that a significant amount of damping was achieved on the modes labeled 1, 3, 4, and 5. Table 4.1 illustrates the effect of the PZTs on the test plate in terms of percent reduction and dB reduction. The results show that a 22 dB reduction was achieved for mode 5 at 245 Hz. It is, however, worth noting that the results shown in Table 4.1 compare the unshunted plate with the undamped plate with no

PZTs attached. Thus, a good portion of the dB reduction achieved by the shunting technique was due to the application of the PZTs to the test plate.

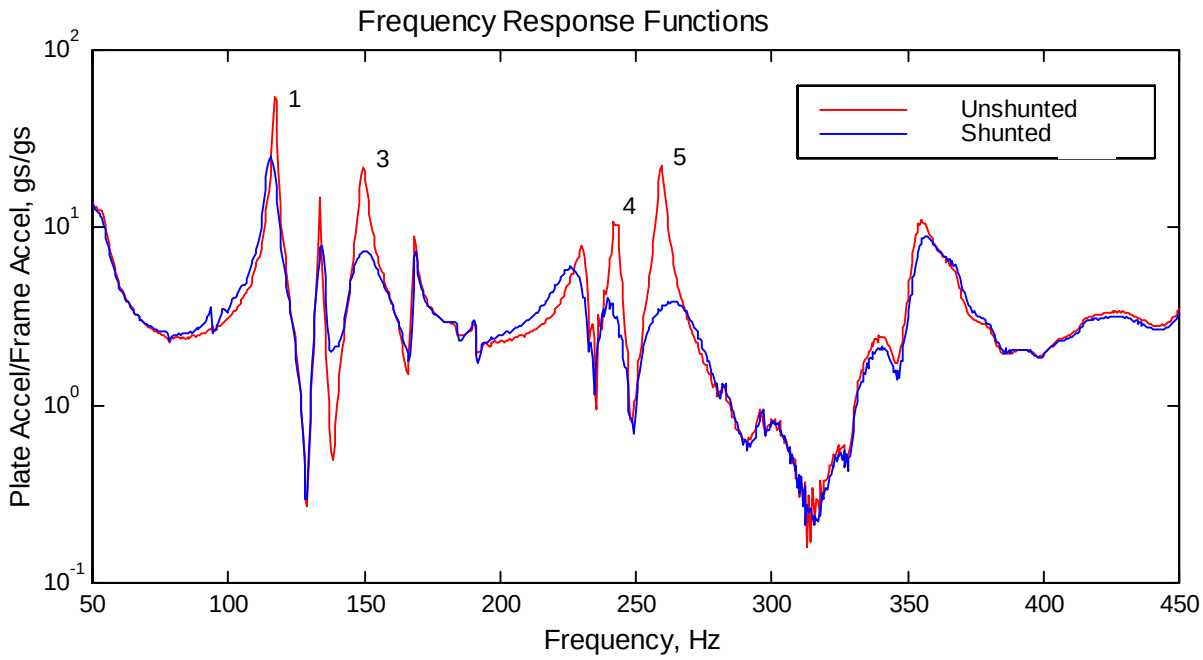

Figure 4.15. Shunted and Unshunted Plate Frequency Response [1]

Table 4.1. Effect PZTs Using Shunt Circuits

Peak	Undamped (g/g)	Shunted PZT (g/g)	Reduction (%)	Reduction (dB)
1 (101 Hz)	57.79	31.84	56.1	5.2
3 (147 Hz)	47.74	7.53	84.6	16.0
4 (235 Hz)	11.28	4.05	64.1	8.9
5 (245 Hz)	47.97	3.87	91.9	21.9

4.3 Positive Position Feedback (PPF)

The control law used for the feedback control system was positive position feedback. Positive position feedback is a relatively new technique for vibration suppression that uses a displacement measurement to accomplish control. PPF control is a stable and relatively simple control method for vibration suppression [24]. The control law for a PPF controller consists of two equations, one describing the structure and one describing the compensator, as shown in equations (2.3) and (2.4) and again in equations (4.1) and (4.2) below.

$$\frac{d^2}{dt^2}(\xi) + 2\cdot\zeta\cdot\omega\cdot\frac{d}{dt}(\xi) + \omega^2\cdot\xi = g\cdot\omega^2\,\eta \quad \longleftarrow \text{Structure} \tag{4.1}$$

$$\frac{d^2}{dt^2}(\eta) + 2\cdot\zeta_f\cdot\omega_f\cdot\frac{d}{dt}(\eta) + \left(\omega_f\right)^2\cdot\eta = \left(\omega_f\right)^2\cdot\xi \quad \longleftarrow \text{Compensator} \tag{4.2}$$

In equations (4.1) and (4.2), g is the scalar gain>0, ξ is the modal coordinate, η is the filter coordinate, ω and ω_f are the structural and filter frequencies, respectively, and ζ and ζ_f are the structural and filter damping ratios, respectively. The positive position terminology in the name PPF comes from the fact that the position coordinate of the structure equation is positively fed to the filter, and the position coordinate of the compensator equation is positively fed back to the structure. The block diagram of a PPF filter can be seen in Figure 4.16. Essentially, a PPF controller behaves much like an electronic vibration absorber, which is tuned to a frequency to absorb vibration energy.

In the design of each PPF filter, there were four parameters that were chosen: the sampling time (*Ts*), the filter damping ratio (ζ_f), the filter gain (k), and the filter frequency (ω_f). The following sections will focus on how each of these parameters was chosen in the design of the PPF controller.

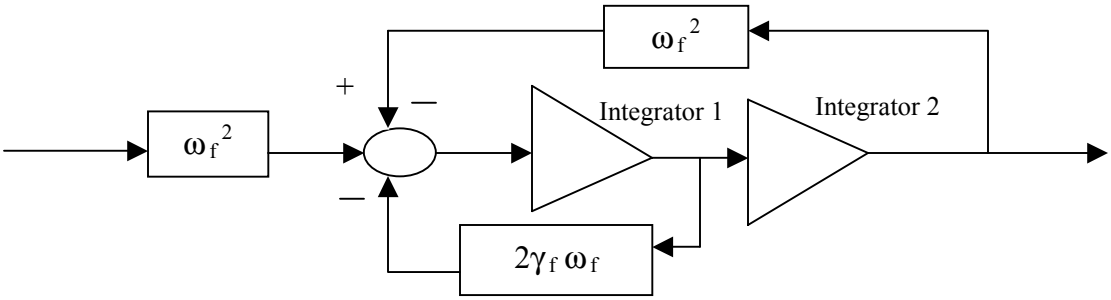

Figure 4.16. Block Diagram of PPF Filter

4.3.1 PPF Filter Frequency Selection

The frequency of each PPF filter was chosen slightly above (approximately 1.2 to 1.5 times) the resonant frequency to be controlled. For example, the PPF filter designed to control the first resonant frequency at 47 Hz was tuned to a frequency between 60 Hz and 70 Hz. Ultimately, however, the frequency of each PPF filter was chosen experimentally based on what frequency gave the best results, or added the most damping to the plate.

The frequency of each filter was often dependant on the number of filters in the controller and the number of modes targeted for control. Experimentally, it was determined that the value of the frequency of each PPF filter was more important as the number of filters in the controller was increased. This has to do with the number of poles that are placed in the Z-plane and the way each of the filter poles roll off. When the continuous PPF filter is converted to discrete-time, the stable region goes from the left half of the S-plane to just inside of the unit circle in the Z-plane. Moreover, the poles were placed in a small area just inside of the unit circle because each filter was converted to the Z-plane with the same sampling period. Thus, the number of PPF filters affected the stability and performance of the overall PPF controller.

Another aspect of each filter frequency was that the higher frequency filters could affect the lower frequency filters. This is especially true when the filters are relatively close in frequency. This phenomenon is due to the fact that PPF filters are second order and have two-pole roll off, which affects lower frequency dynamics more than higher frequency dynamics. For example, one of the PPF filters was designed to control the resonant frequency at 150 Hz. If the filter frequency was chosen at or slightly higher

than 150 Hz, this PPF filter could add damping to the mode at 150 Hz and each mode lower than this frequency.

4.3.2 PPF Filter Damping and Sampling Time Selection

The damping of each PPF filter was chosen experimentally based on the range of values that worked best. In fact, for almost every PPF filter the damping coefficient was chosen between 0.01 and 0.1. Values greater than 0.1 did not add as much damping to the plate and in some cases produced unstable controllers. The damping coefficient was chosen and usually kept constant throughout the controller design process.

The sampling time of each PPF filter was used to convert the continuous state-space controller to a digital controller. Experimentally, it was determined that sampling rates between 1,000 Hz and 10,000 Hz gave the best results. It is worth noting that for most of the PPF controllers a sampling rate of 1,000 Hz was used.

4.3.3 PPF Filter Gain Selection

The selection of the filter gains was perhaps the most important part of the PPF controller design. If the gains were chosen incorrectly then the controller was often unstable or added little or no damping to the targeted resonant frequencies. The design process for a multiple PPF filter controller with multiple gains requires a top down approach. Since it is not possible to vary the PPF filter gains simultaneously, the filters are tuned one at a time. The controller is designed from the highest frequency filter to the lowest because of the two-pole roll off of each filter, which affects lower frequencies more than higher frequencies.

The following example describes how a five PPF filter controller was designed to control five modes of the test plate. Before any of the parameters were chosen for the filters, the gains for each of the four lower frequency PPF filters were set to zero. It should be noted that each filter was initially designed to control only one mode of the test plate. Figure 4.17 shows a block diagram description of the PPF filters and gains to help

explain the initial design procedure for a PPF controller. In the highest frequency filter, as shown in Figure 4.17, the frequency and the gain were initially chosen to control the mode at 370 Hz. The frequency and the gain were varied until a maximum level of damping was obtained. Once the parameters of the 370 Hz filter were chosen, the second highest filter (the 253 Hz filter) was designed around the closed loop system of the structure and the first filter. The same 'top-down' approach was used until the 47 Hz filter was designed. If for instance the procedure was performed from the lower frequency filters first, the dynamics of the higher frequency filters would affect the lower frequency filter's design specifications. Another advantage to this 'top-down' design approach is the lowest frequency structural pole will always go unstable if the filter gains are too large. After each filter was designed, a fine-tuning process was used to optimize the overall control authority of the PPF controller. The fine-tuning process included making minor adjustments to the filter gains and frequencies.

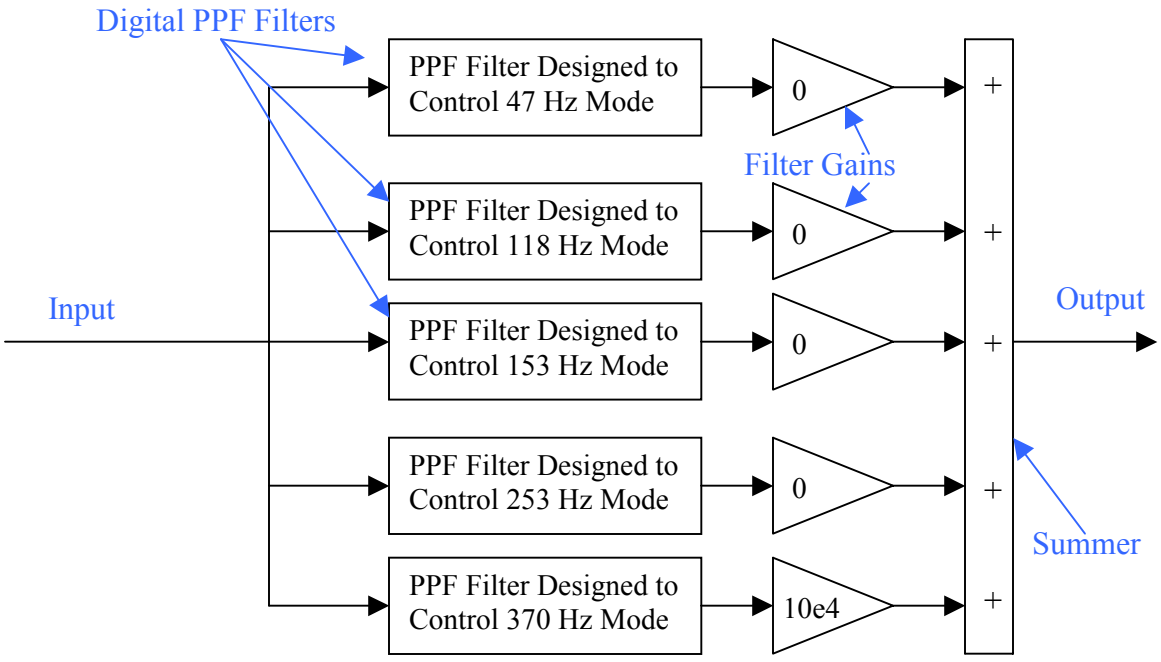

Figure 4.17. Block Diagram of PPF Controller

4.4 Active Control Testing and Results

The purpose of this section is to present the testing methods and the results obtained for the active control tests conducted on the test stand. This section also includes a discussion of the feedback control law used for the control system and the hardware used to implement the control. In the active control tests, the frequency range used to excite the undamped test plate was 0-400 Hz. This frequency range was used for the baseline tests because the active control testing did not include an acoustic analysis. Therefore, the comparison made between the shunted PZT and active control tests in Chapter 5 will focus on the 50-400 Hz frequency range.

4.4.1 dSPACE and Simulink Block Diagram

The block diagram for the PPF filter and for the rest of the control system was setup in Matlab's Simulink Toolbox, in conjunction with a dSPACE control board. Simulink is a graphical program that allows the user to input a block diagram and generate the corresponding ANSI C-code. The C-code is generated from Matlab's target files, which specify the particular code for each block used in the Simulink model. The control system's Simulink block diagram can be seen in Figure 4.18. Each block in Figure 4.18 corresponds to a particular part of the control system. The block at the far left, labeled DS1102ADC, and at the far right, labeled DS1102DAC, are the analog to digital and the digital to analog converters, respectively. The two blocks labeled Discrete Transfer Function 1 and Discrete Transfer Function 2 are high-pass filters, which eliminate any DC-offset that the optical fiber sensor may contain. The Discrete State Space blocks contain the PPF filters for each mode of the representative aircraft panel that needs to be controlled (See Figure 4.16 for the model of each PPF filter). The active control system was designed by tuning each PPF filter to control one or more of the modes of the representative aircraft panel. The entire control system block diagram can be seen in Figure 4.19, which shows how the Simulink model and dSPACE board fit into the control system. The control system was set up such that the optical fiber sensor sends a signal through a signal conditioner and amplifier into the dSPACE board. Once the signal was

processed through the PPF control law it was sent out to an amplifier to drive the PZT actuator.

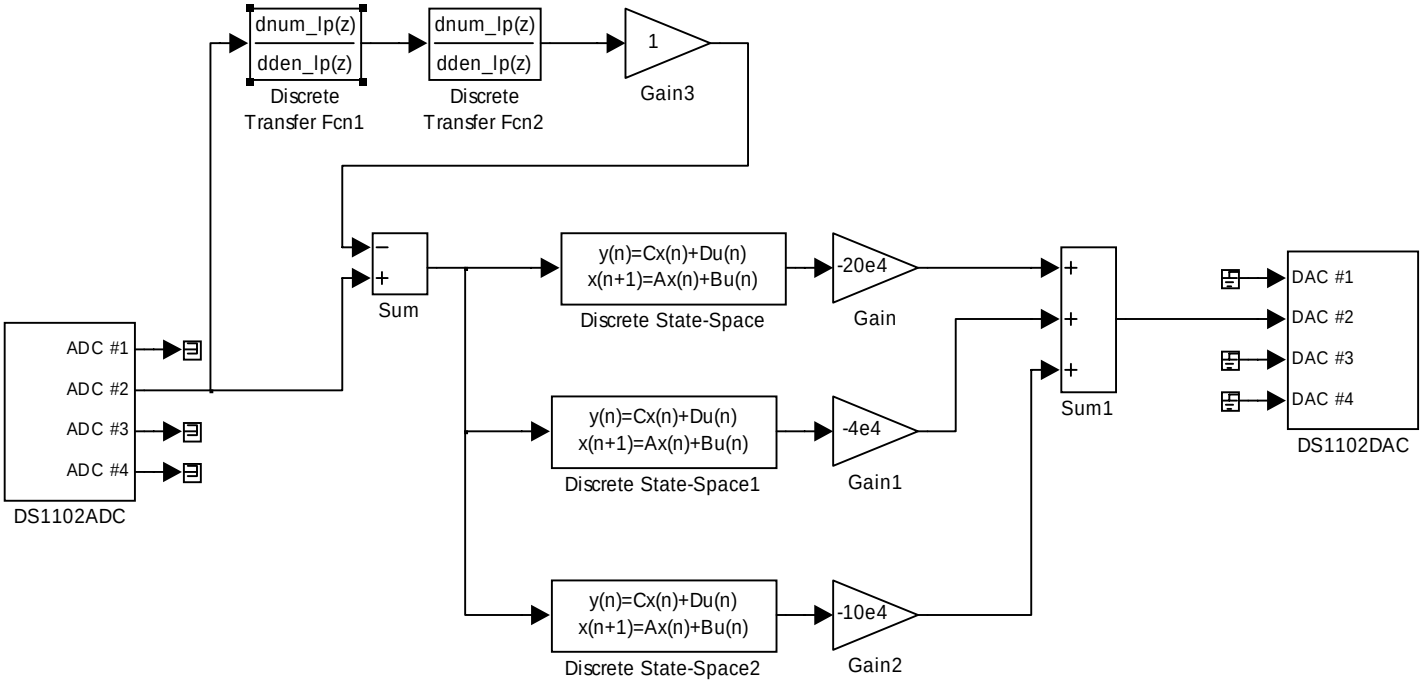

Figure 4.18. Simulink Block Diagram

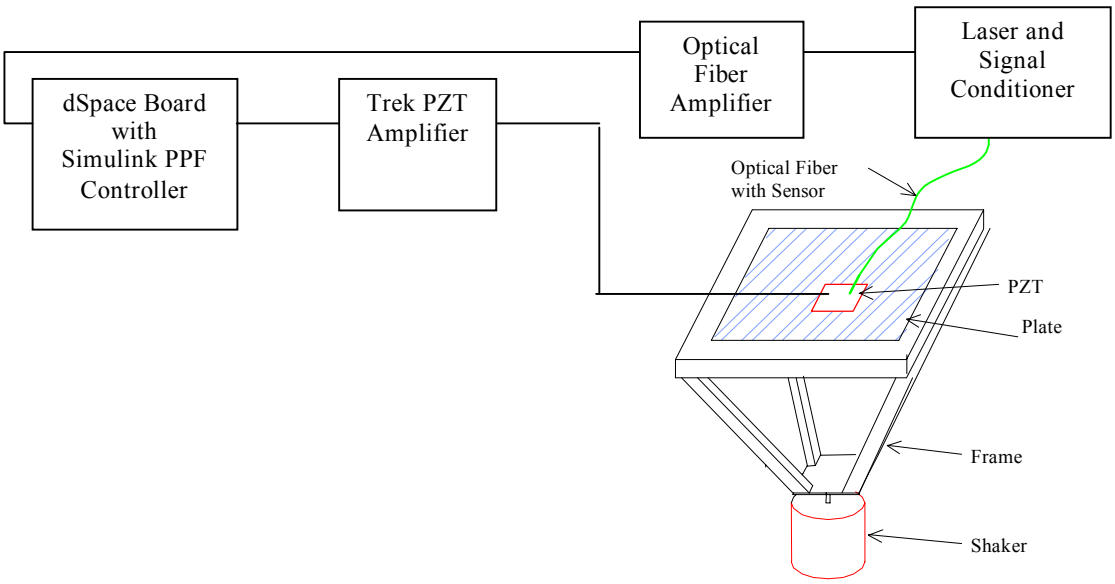

Figure 4.19. Control System Block Diagram

The system's parameters and the overall control system's performance were measured using a two channel HP Dynamic Signal Analyzer. This signal analyzer was used to get the frequency response function between the plate and the clamping frame using two accelerometers, one on the bottom center of the plate and one on the clamping frame, as described in Section 3.2.3. A complete system block diagram showing the overall test setup can be seen in Figure 4.20 on the next page.

The active control tests were conducted in a controlled environment in the Advanced Vehicle Dynamics Laboratory (AVDL) at Virginia Tech. The procedure for the active control tests was as follows:

1. Turn on the equipment (PC, HP Analyzer, Amplifiers, and Signal Conditioners).
2. Set the HP Dynamic Signal Analyzer for two channels, uniform window, anti-aliasing filter on, 20 averages, span of 400 Hz, periodic chirp input, and 800 spectral lines.
3. Set the gain on the Trek 50/750 PZT amplifier to 100.
4. Set the gain on the PCB signal conditioner at 10 for both channels.
5. Set the filter frequency and the damping ratios for the PPF filters in the Simulink model.
6. Turn on the shaker and the controller.
7. Take data on the HP Dynamic Signal Analyzer.

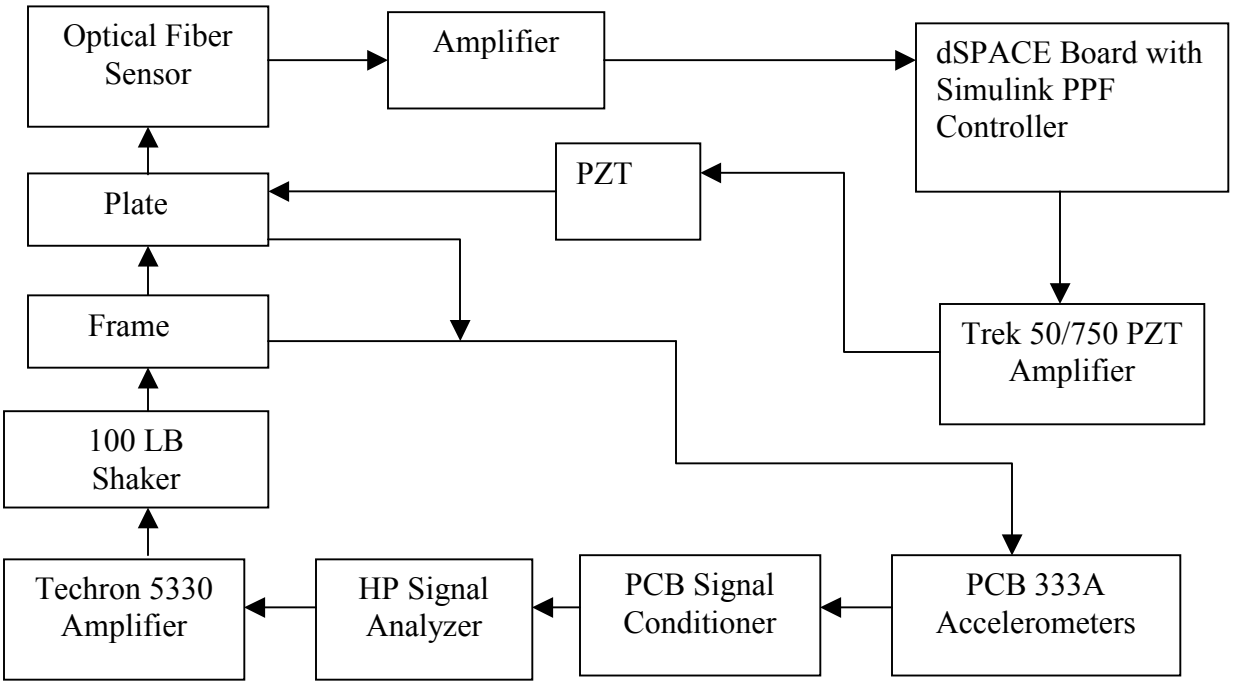

Figure 4.20. Active PZT Test Setup

4.4.2 Active PZT Test Results

A series of tests were run to determine the optimum parameters for the active vibration suppression of a representative aircraft panel. These parameters, ranging from the gains assigned to the various amplifiers to the damping ratios of the PPF filters, were based upon the tuned frequency and the number of modes assigned to each PPF filter. Figure 4.18 showed one of the Simulink Models used for the active control tests. This model uses three PPF filters to provide active damping to most of the modes from 0-400 Hz. One, however, can achieve significant active damping of a mode or modes with as few as one PPF filter, tuned properly.

There were two different means of supplying energy to the plate for the active control tests. The first method used a 100 lb shaker to excite the plate mechanically, and the second method used a 10 in. sub-woofer to excite the plate acoustically. Both the

shaker and the speaker were driven with a 0-400 Hz periodic chirp input signal, which is shown in Figures 3.15 and 3.16.

The initial design procedure for the active control system was to create a Simulink model with one PPF filter to control as many modes as possible. This design method involved determining the frequency range at which the system had control authority over multiple modes. The tests results show that the control system with one PPF filter was most effective when tuned to a frequency between 60 and 70 Hz, just above the fundamental mode of the plate. Figures 4.21 and 4.22 show some of the best results obtained with the one PPF filter controller. In each of these tests the 100 lb shaker excited the plate mechanically.

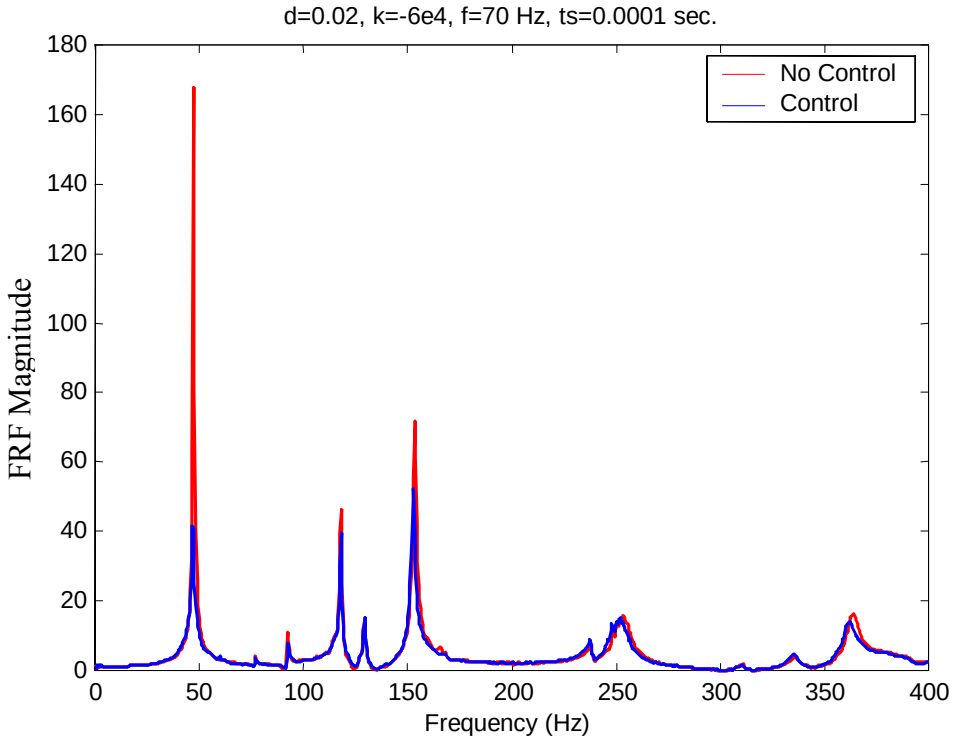

Figure 4.21. Active Control with 1 PPF Filter (Mechanically Excited)

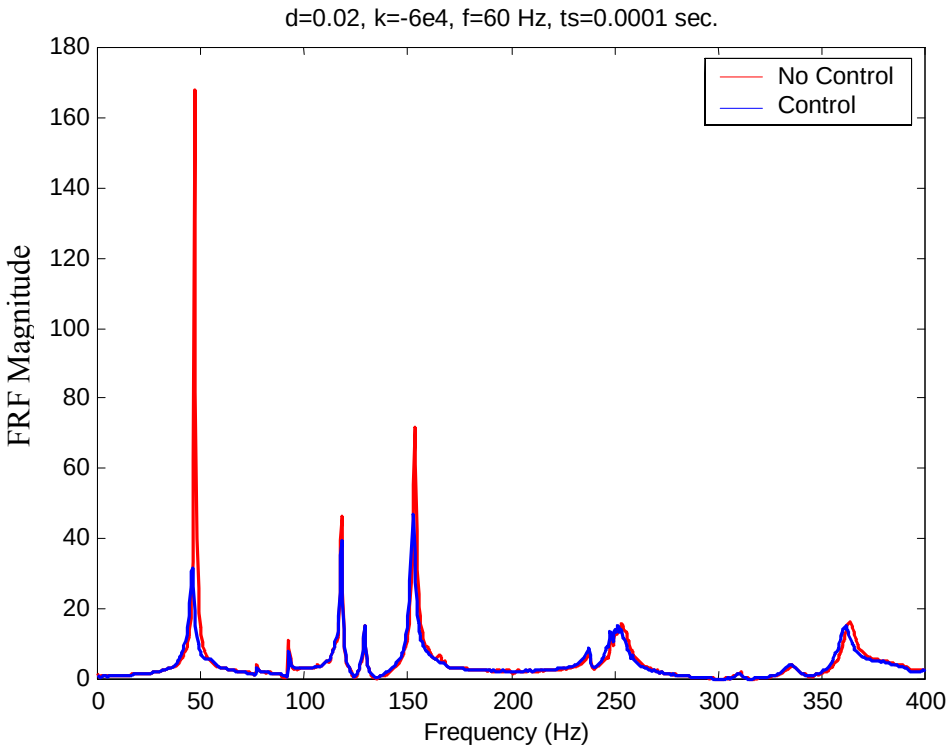

Figure 4.22. Active Control Test with 1 PPF Filter (Mechanically Excited)

The parameters listed at the top of each of these figures represent the parameters used for the active control system. The active control test shown in Figure 4.21 was run with a PPF filter damping ratio of 0.02, a Simulink gain of –60,000, a sampling time of 0.0001 seconds, and tuned to a frequency of 70 Hz. The active control test shown above in Figure 4.22 was run with the same parameters as the test shown in Figure 4.21, except the filter was tuned for 60 Hz. These figures show that the control authority of the first mode is increased as the frequency of the PPF filter approaches the frequency of the first mode, 47 Hz. It should be noted that as the frequency of the PPF filter was decreased to below 60 Hz, the control authority of the higher modes was also decreased.

In the acoustic tests, a 10 in. sub-woofer was placed just under the center of the plate, approximately 2 inches away. The plate was excited with the same 0-400 Hz periodic chirp input signal, however, the frequency response function had to be taken differently. Instead of taking the input as the frame accelerometer, the input of the frequency response function was changed to the generated input signal to the speaker. Figure 4.23 shows the results obtained with a one PPF filter controller when the plate was excited acoustically with a 10 in. sub-woofer. The active control test shown in Figure

4.23 was run with a PPF filter damping ratio of 0.02, a Simulink gain of –80,000, a sampling time of 0.0001 seconds (10,000 Hz), and tuned to a frequency of 60 Hz.

Additional tests were run using pure tone inputs at the resonant frequencies of the plate. These tests were performed to determine the effectiveness of the controller in the suppression of the structure born noise resulting from the vibration of the test plate. Most of these tests were run at the first resonant frequency of the plate (47 Hz) because this mode produced the most audible structure born noise. The test results proved that the controller reduced the noise from the plate significantly. Figure 4.24 shows the best reduction achieved by the controller with a 47 Hz pure tone input signal.

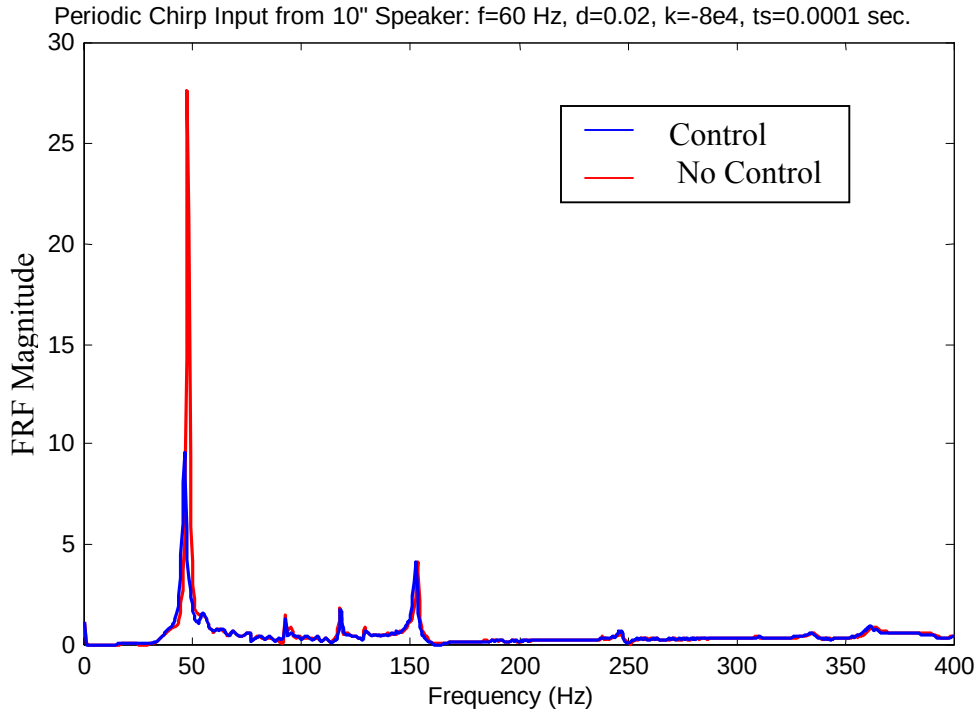

Figure 4.23. Active Control Test with 1 PPF Filter (Acoustically Excited)

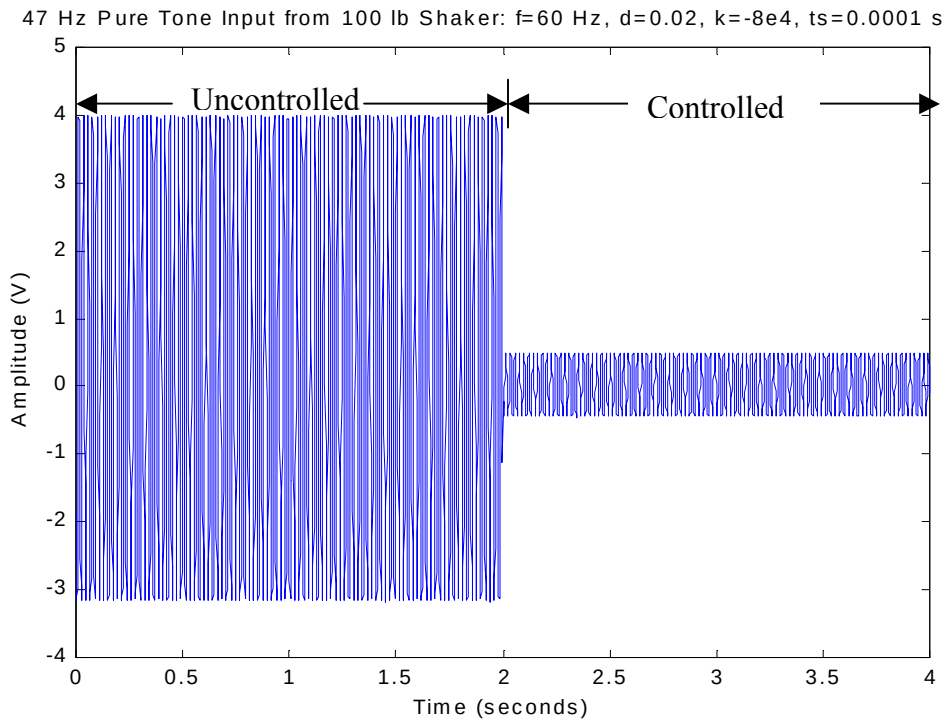

Figure 4.24. 47 Hz Pure Tone Active Control Test

One of the final controller designs used three PPF filters to attack multiple modes in the 0-400 Hz frequency range. This controller has an advantage over the one PPF filter controller because it can be tuned to three frequencies and, therefore, have more control authority over the structure. Figure 4.25 shows some of the best results obtained with the three PPF filter controller.

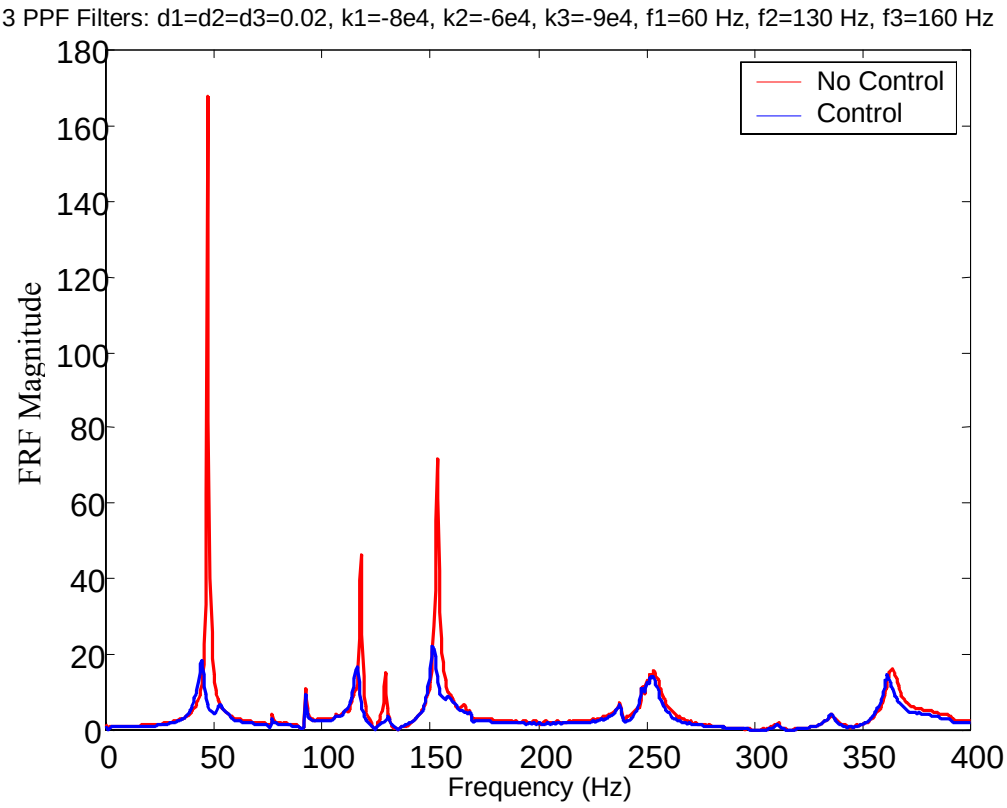

Figure 4.25. Active Control Test Results with 3 PPF Filters

The parameters listed at the top of Figure 4.25 correspond to the damping ratios, the Simulink gains, and the frequencies of the three PPF filters, respectively. The results from this figure show that the three PPF filter controller can achieve a reduction in the first mode of the uncontrolled plate up to 90% with an added weight of only 0.04 lb of piezoelectric material.

More complex control systems were designed with up to six PPF filters to investigate the advantages of attacking more modes. Figure 4.26 and 4.27 show some of the best results obtained with 5 PPF filters. The parameters used for the system shown in Figure 4.26 are: $\zeta_1=\zeta_2=\zeta_3=\zeta_4=\zeta_5=0.02$, $f_1 = 65$ Hz, $f_2 = 140$ Hz, $f_3 = 145$ Hz, $f_4 = 170$ Hz, $f_5 = 280$ Hz, and $k_1 = -20e4$, $k_2 = -5e4$, $k_3 = -30e4$, $k_4 = -20e4$, $k_5 = -40e4$; where ζ_1, ζ_2, ζ_3, ζ_4, and ζ_5 are the PPF filter damping ratios; f_1, f_2, f_3, f_4, and f_5 are the PPF filter frequencies; and k_1, k_2, k_3, k_4, and k_5 are the PPF filter gains. The parameters used for the system shown in Figure 4.27 are: $\zeta_1=\zeta_2=\zeta_3=\zeta_4=\zeta_5=0.02$, $f_1 = 65$ Hz, $f_2 = 140$ Hz, $f_3 = 145$ Hz, $f_4 = 170$ Hz, $f_5 = 280$ Hz, and $k_1 = -20e4$, $k_2 = -5e4$, $k_3 = -20e4$, $k_4 = -20e4$, $k_5 =$

-40e4. With 5 PPF filters, reductions in the first mode were achieved up to 95 % of the uncontrolled plate value. However, with changes in the optical fiber sensor, or the boundary conditions of the plate, the control system would sometimes experience stability problems. The three PPF filter controller had better system stability. In addition, the three PPF filter controller was more robust to changes in the optical fiber sensor or boundary conditions of the plate. Table 4.2 shows the results obtained in the active control tests in terms of percent reductions and dB reductions. It should be noted that these results were obtained using only the center PZT as the actuator. The results of Table 4.2 show the bandwidth of control using active control with positive position feedback.

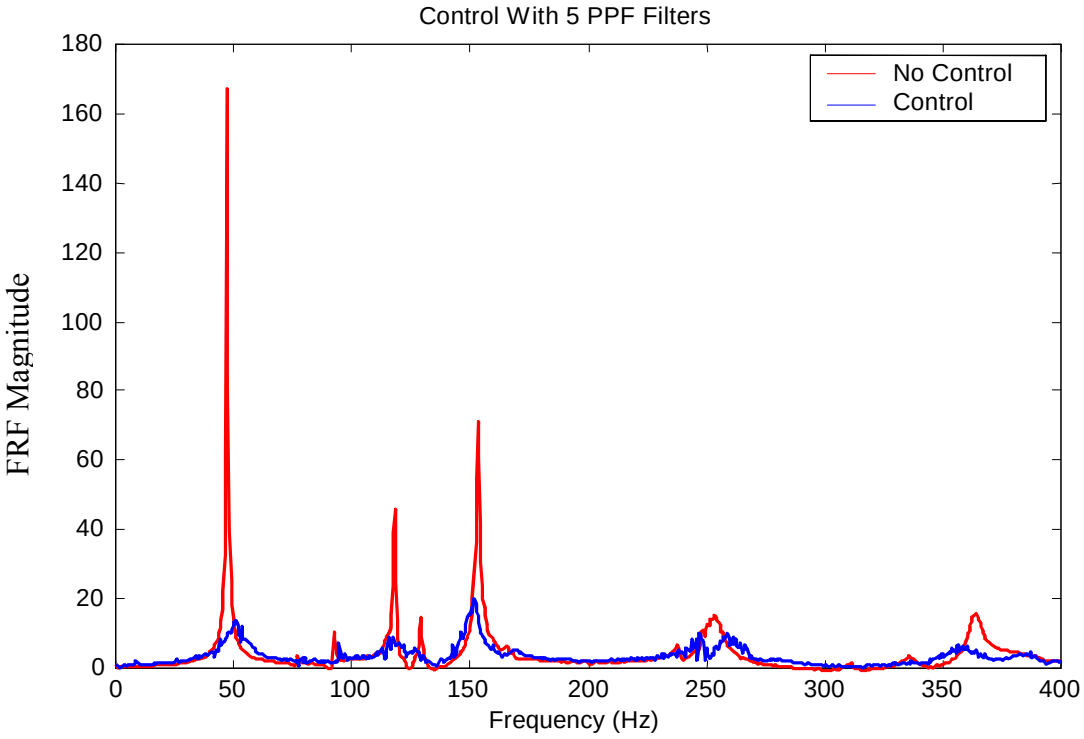

Figure 4.26. Control With 5 PPF Filters

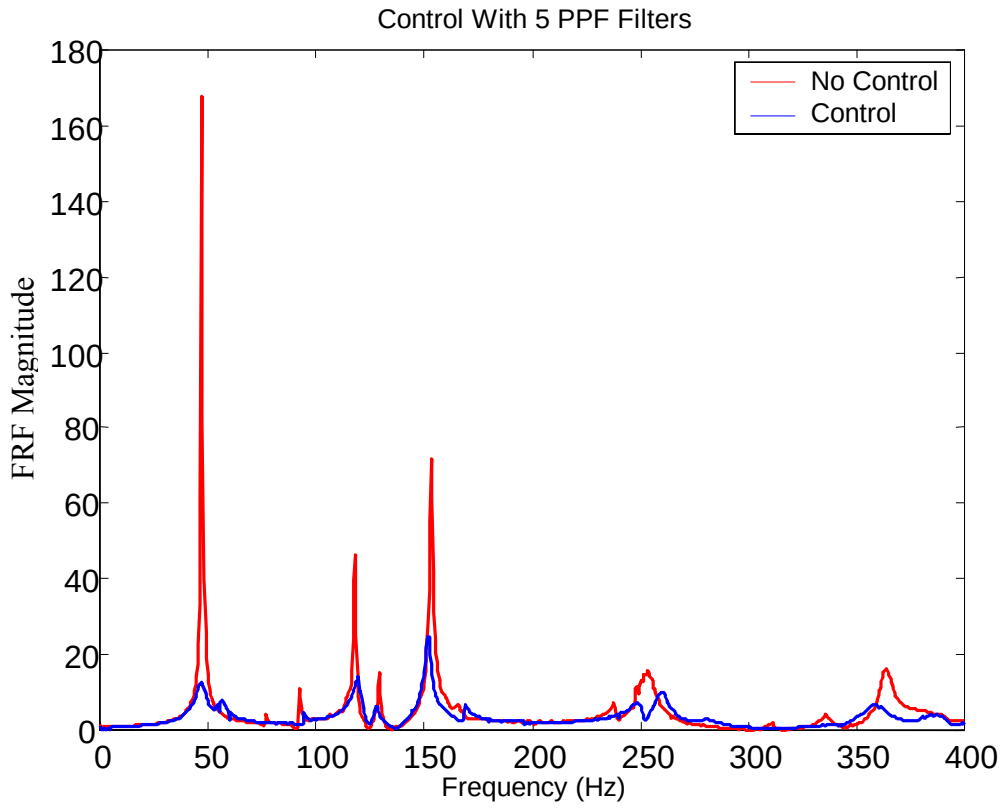

Figure 4.27. Control With 5 PPF Filters

Table 4.2. Effect of Actively Controlled PZTs on Plate Vibration Levels

Peak (Hz)	Undamped Plate (g/g)	Uncontrolled Plate (g/g)	Controlled Plate (g/g)	Reduction from Undamped Plate (dB)	Reduction from Uncontrolled Plate (dB)
47	110	168	12.39	19	22.7
118	88	46.5	14	16	10.4
153	114	72	21.9	14.3	10.3
253	56	15.7	9.7	15	4.2
370	17	16.5	6.7	8	7.8

Additional tests were conducted on the test plate to develop an online damage detection system for health monitoring. This health monitoring system uses an impedance method to detect damage such as a loose bolt in the clamping frame. The

following section describes this method in detail and presents some of the results obtained.

4.5 Impedance-Based Health Monitoring Technique

This section describes the impedance-based health monitoring technique developed for the active control system. This technique was used in conjunction with the active control system to provide simultaneous control and health monitoring of the test plate. Also, this section presents the experimental results with health monitoring and temperature effects.

4.5.1 Impedance Method

A new smart health monitoring technique capable of on-line incipient damage detection in complex structures was employed after an extensive search of possible damage detection methods. The basic concept of this impedance-based structural health monitoring technique is to monitor the variations in the structural mechanical impedance caused by the presence of damage. Since structural mechanical impedance measurements are difficult to obtain, this non-destructive evaluation technique utilizes the electromechanical coupling property of piezoelectric materials.

This health monitoring method uses one PZT patch for both the actuating and sensing of the structure's response. A simple impedance model can describe the interaction of a PZT patch with the host structure. Figure 4.28 presents the elements of the model. The PZT is considered as a thin bar undergoing axial vibrations in response to the applied sinusoidal voltage.

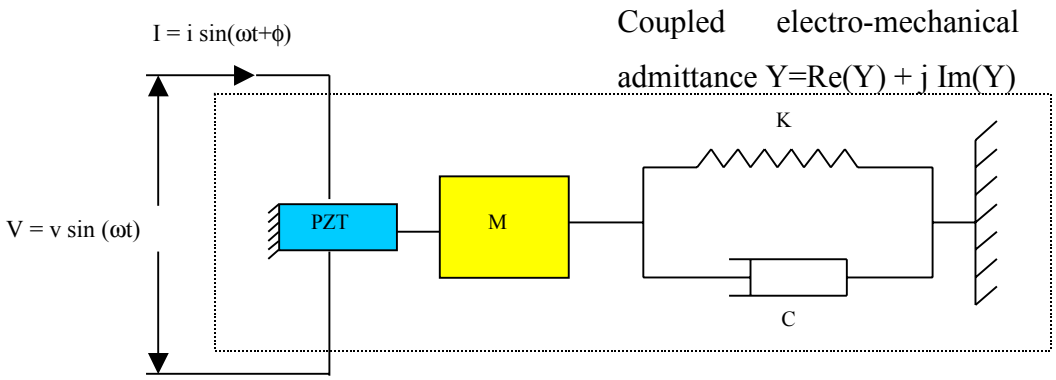

Figure 4.28. 1-D Model Used to Represent a PZT-Driven Dynamic Structural System

Solving the equation for the PZT bar connected to the external mechanical point impedance of the structure leads to Equation (4.3) for the frequency dependent complex electrical admittance Y(ω) (inverse of impedance). The variables Z_a and Z_s represent the PZT's and the structure's mechanical impedance, respectively. $\hat{Y}_{xx}^{E}$ is the Young's modulus of the PZT at zero electric field, d_{3x} is the piezoelectric coupling constant in an arbitrary x-direction at zero stress, ε_{33}^{T} is the dielectric constant at zero stress, δ represents the dielectric loss tangent of the PZT, and *a* is the geometric constant of the PZT. Equation (4.3) clearly indicates the direct relation of the mechanical impedance of the structure to the electrical impedance bonded onto this structure.

$$Y(\omega) = i\omega a\left(\bar{\varepsilon}_{33}^{T}(1-i\delta) - \frac{Z_s(\omega)}{Z_s(\omega)+Z_a(\omega)} d_{3x}^{2}\hat{Y}_{xx}^{E}\right) \qquad (4.3)$$

Damage in the structure is reflected in changes of the parameters such as mass, stiffness, or damping. Assuming that the PZT's parameters remain constant, any changes in the mechanical impedance Z_s change the overall admittance. Previous Experiments in the laboratories have shown that the real part of the overall impedance contains sufficient information about the structure, and is more reactive to damage, than the magnitude or the imaginary part. Therefore, all impedance analyses are confined to the real part of the complex impedance. The actual health monitoring was done by saving a healthy impedance signature of the structure and comparing this signature with other signatures taken over the structure's service life.

4.5.2 Implementing the Non-Destructive Experiments in the Test Setup

Initial laboratory tests on the uncontrolled plate showed the ability of the impedance method to detect certain forms of damage on the plate. The tests used the same PZT patches as for the control system. The impedance measurements were taken with an HP 4194A Impedance Analyzer. A frequency range of 45 kHz to 55 kHz proved to be optimum for detecting damage in this structure. To simulate damage on the plate one or two bolts of the clamping frame were loosened from 25 ft-lb. to 10 ft-lb. Figure 4.29 shows a sketch of the frame and names the bolts that were loosened. Adding mass to the test specimen could not be used to simulate damage, because the mechanical impedance is mostly defined by the boundary conditions of the clamped plate.

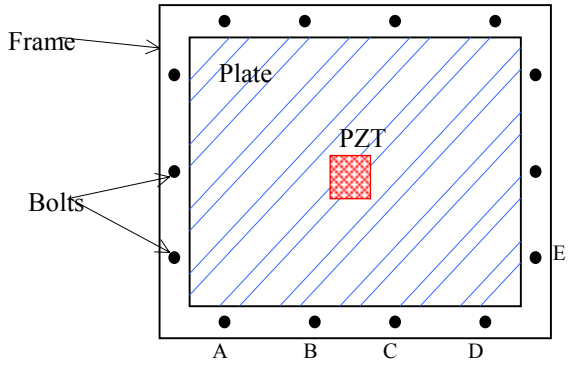

Figure 4.29. Clamping Frame with Bolts [28]

Since the task consisted of simultaneous health monitoring and active control, the actuators for both the control and the health monitoring system needed to be de-coupled. The impedance method is very sensitive to disturbing voltages in the measuring circuit. The controller however creates exactly those disturbances by generating the control signal. A simple capacitor of 390 nF in series with the impedance analyzer blocked the control signal from the impedance analyzer. The block diagram of the test setup is presented in Figure 4.30. All health monitoring data presented in this report was taken while the shaker was exiting the plate with a periodic chirp signal from 0 to 200 Hz. The active controller was also switched on and increased the damping of the first three modes of the plate significantly.

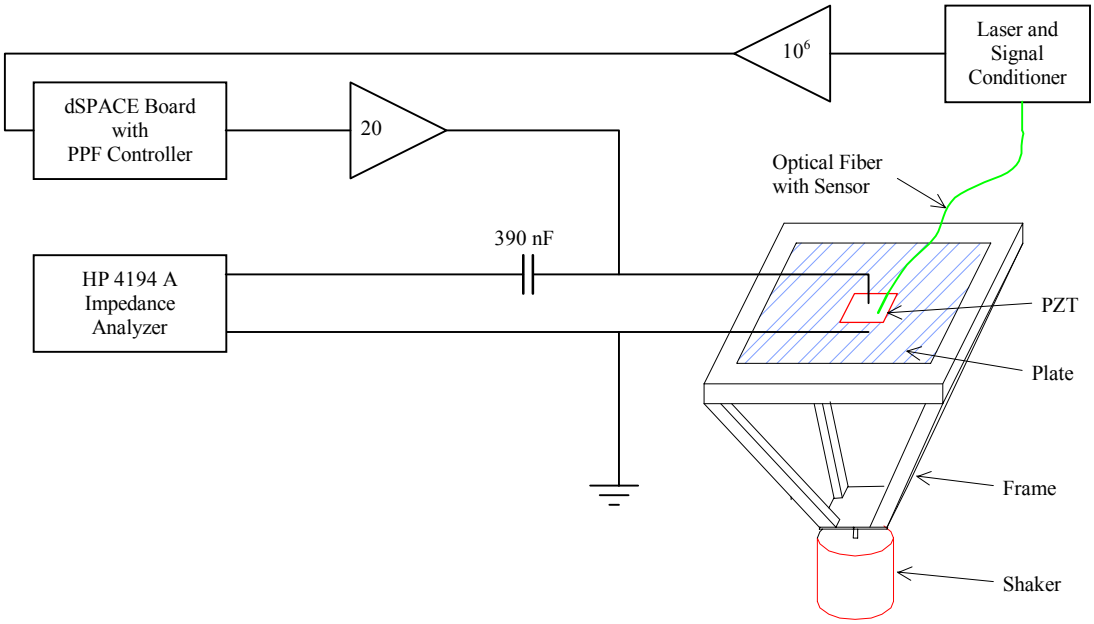

Figure 4.30. Block Diagram of the Test Setup: Health Monitoring and Active Control

4.5.3 Health Monitoring Results

Figure 4.31 shows the impedance signatures of the undamaged and damaged plate. To simulate damage the bolts B and C were loosened to 10 ft-lb of torque from 25 ft-lb. The signature change is significant because both bolts are very close to the PZT patch. For comparing impedance signatures, a qualitative damage assessment has been developed. The assessment is made by computing a scalar damage metric, defined as the sum of the squared differences of the real impedance at every frequency step. Equation 4.4 gives the damage metric M in a mathematical form. The used variables include: $Y_{i,1}$ the healthy impedance at the frequency step i, $Y_{i,2}$ the impedance of the structure after the structure has been altered, and n the number of frequency steps.

$$M = \sum_{i=1}^{n} \left[\mathrm{Re}(Y_{i,1}) - \mathrm{Re}(Y_{i,2}) \right]^2 \qquad (4.4)$$

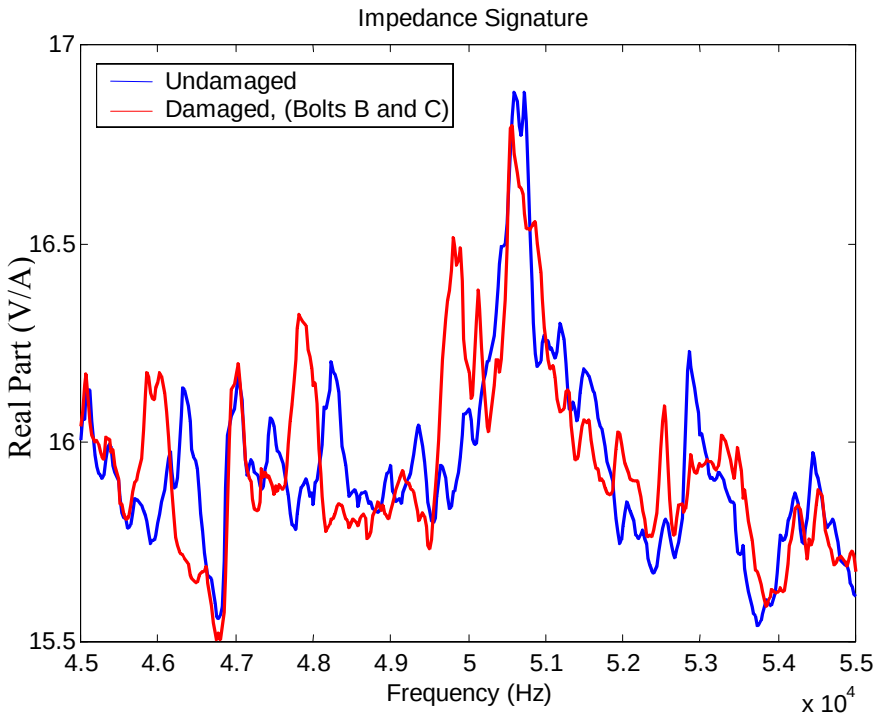

Figure 4.31. Impedance Signatures for the Undamaged and Damaged Test Plates [28]

The damage metric simplifies the interpretation of the impedance variations and summarizes the information obtained by the impedance curves. Different damage metric values of the plate are presented in Figure 4.32. Note the difference in the metric between one bolt loosened and two bolts loosened. It supports the idea of a damage threshold value to warn an operator when this threshold value has been reached. The chart also illustrates that the closer the damage to the sensor happens the earlier the damage can be detected. Loosening bolts D and E surely represent a similar damage then loosening bolts B and C. However, the damage metric of bolts D and C loosened is smaller than the damage metric of bolts B and C loosened. This is due to the relative distance of the damage to the PZT sensor.

Figure 4.32 also shows a problem with the impedance technique. After re-tightening all bolts back to 25 foot-pounds torque, another set of impedance values was taken and the damage metric was computed. The metric value on the right demonstrates that the impedance signatures from the undamaged plate and the "repaired" plate were noticeably different. The impedance technique is so sensitive that it is almost impossible

to achieve the same impedance signature as before altering after the structure was altered and re-altered.

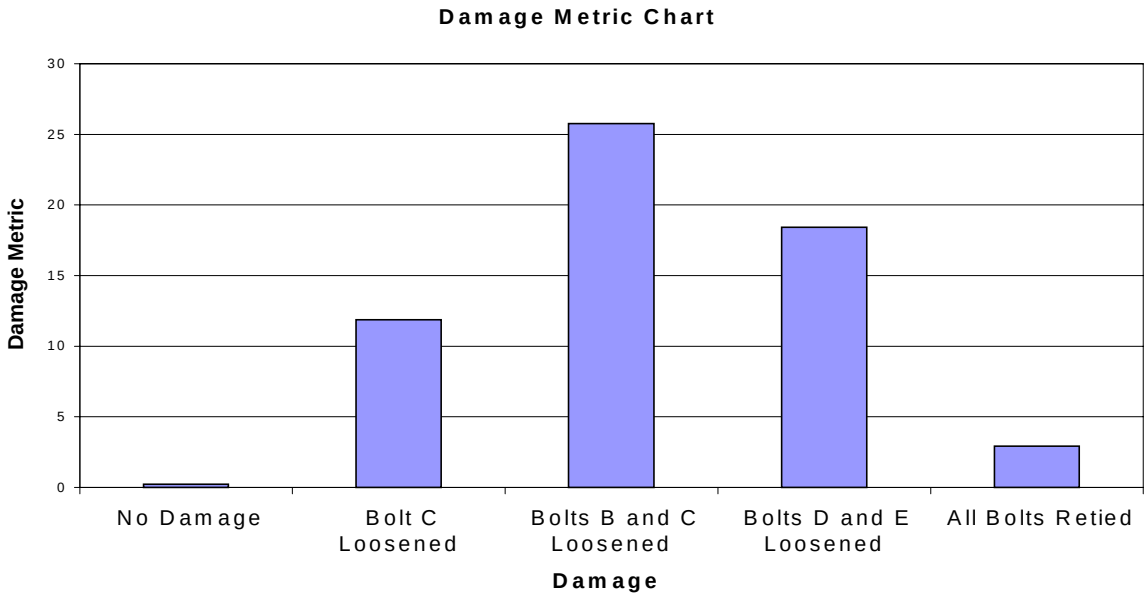

Figure 4.32. Damage Metric Chart of Different Impacts to the Plate [29]

To prove the reliability of the NDE technique several measurements in intervals of several hours were taken. During all measurements, the shaker applied a periodic chirp vibration signal to the plate and the active controller was in operation. No damage was induced to the test specimen while this experiment was run. The results presented in Figure 4.33 show the time elapsed after the first data set was taken. Figure 4.33 also contrasts the repeatability metrics to an actual impact on the structure. The plot shows that there is a slight drift in the scalar damage metric over time due to changing environmental conditions. However, compared to values of the damage metrics of other NDE tests, the drift in the damage metric over time can be neglected.

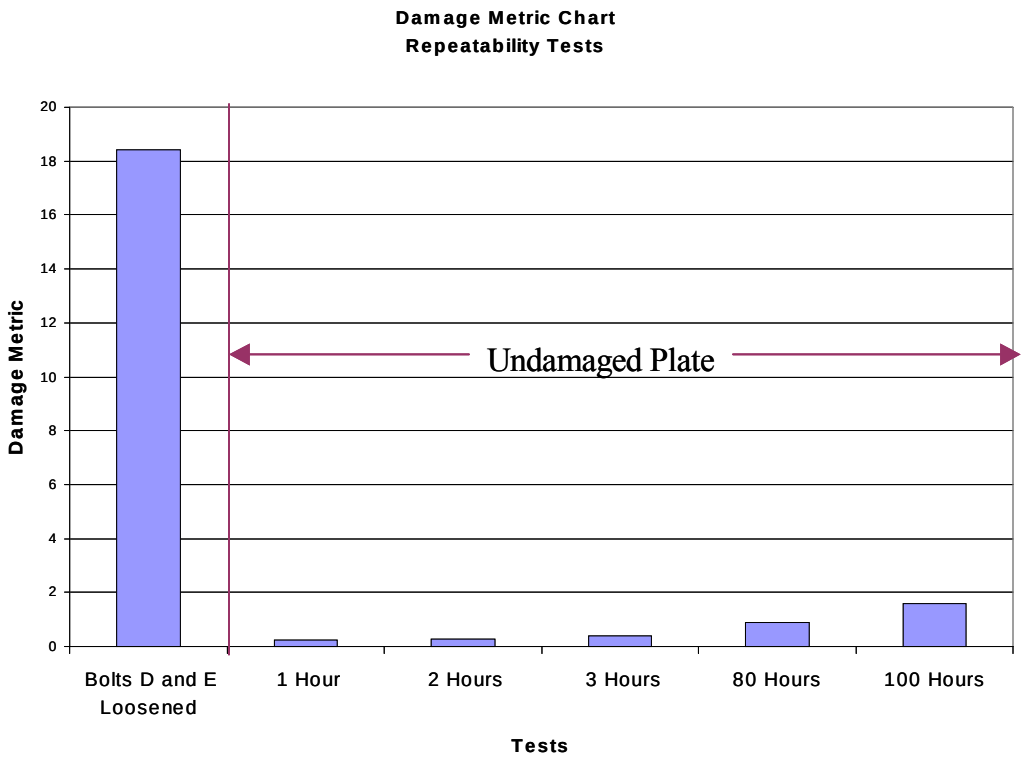

Figure 4.33. Damage Metric Chart -- Repeatability Tests [28]

4.6 Vibration Testing Under Varied Temperatures

This section provides the results obtained for the damage detection system as the temperature of the test plate was varied. These results provide evidence that the control system and optical fiber sensors still provide control as the temperature was varied. This section will also describe the test setup used in for the temperature experiments.

4.6.1 Test Setup

This research included an investigation into whether the active damping with PZTs and fiber optics is effective in a wider temperature range. It is known that properties of the smart materials such as piezoelectric ceramics and optical fibers are temperature

dependent. For instance, the pyroelectric voltage of a PZT changes as the temperature is increased, and the air-gap length of an EFPI sensor might be affected as well.

To show the ability of the active control system to work at a different temperatures an external heat source providing a warm air stream was used. This air stream directed to the center of the plate heated the fiber optic sensor, the PZT actuator, and their surroundings on the plate. A small temperature sensor attached central on the bottom side of the plate measured the temperature of the steel plate at this point. Because steel conducts heat very well, the temperature of the sensor-actuator system could be assumed to be close to the measured temperature. The air stream heated the center of the plate up to 48ºC (118ºF) depending on the power settings on the heat source.

4.6.2 Results

The experiments have shown that the temperature dependent properties of the PZT actuator do not affect the control system. Furthermore, the temperature effects from the fiber optic sensor could be compensated by the same signal processing system as for compensating the drifting DC offset. The control parameters, however, needed to be changed because the heating of areas of the test specimen changed its properties significantly. The first mode of the plate for instance shifted from 47.5 Hz at 22ºC (72ºF) to 154 Hz at 48ºC (118ºF). Figure 4.34 illustrates the results.

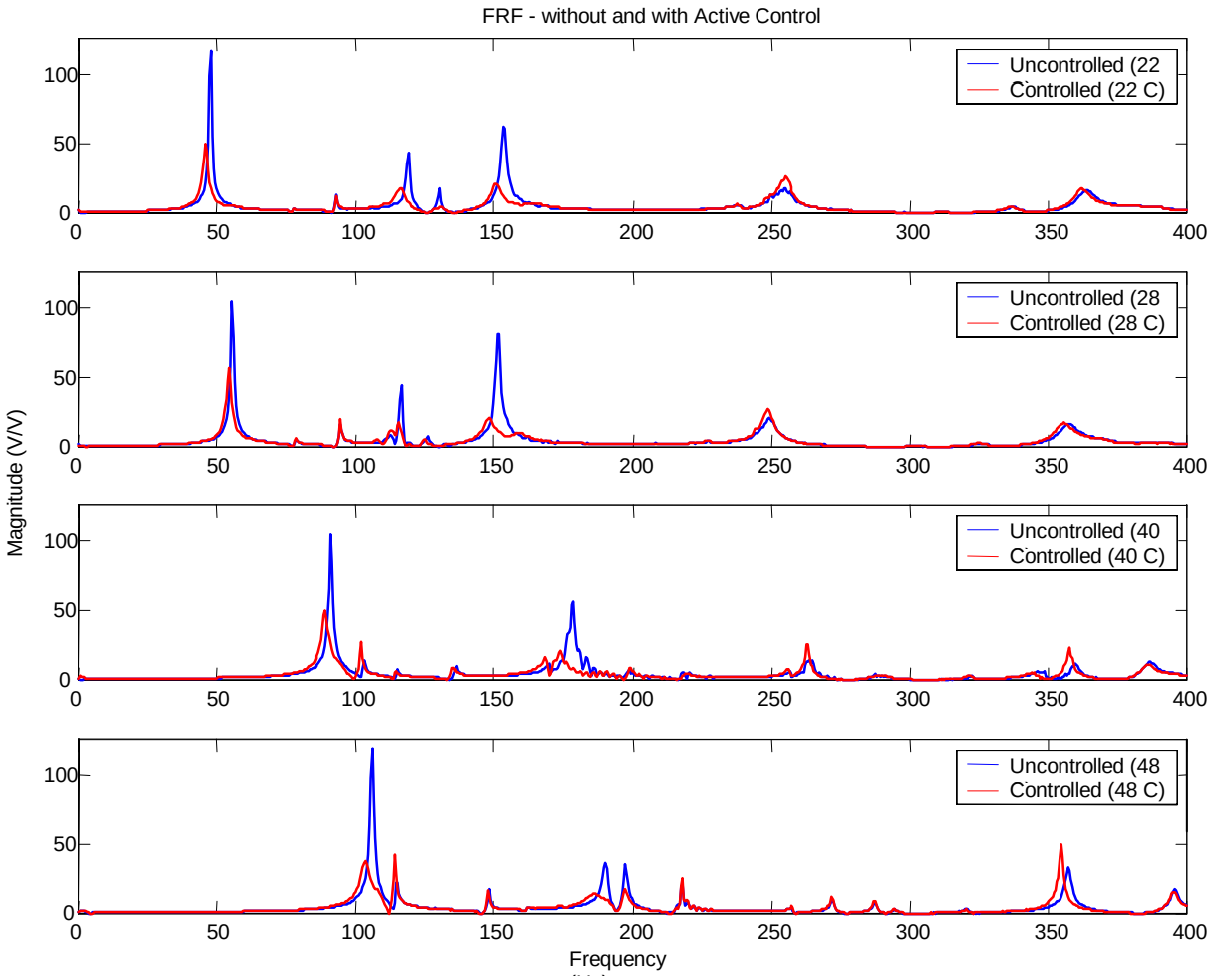

Figure 4.34. Active Control Under Varied Temperatures

The second mode of vibration was significantly decreased at the temperature of 40ºC. The immense changes in the plate's frequency response made adjustments to the control system's parameters necessary. Table 4.3 shows the parameters for the PPF-controller at each temperature point. The variables f_1, f_2, and f_3 stand for the filter frequencies, ζ_1, ζ_2, and ζ_3 are the damping ratios, and k_1, k_2, and k_3 are the gains, respectively.

After adjusting the controller parameters: pole frequencies and amplifying gains the active control was capable to perform as well at higher temperatures than room temperature. Figure 4.33 also shows the frequency response of the plate with the operating active controller modified accordingly. The quantitative results are summarized in Table 4.4.

Table 4.3. Controller Parameters for Different Plate Temperatures [29]

Controller Parameters	Temperature			
	22ºC (72ºF)	28ºC (82ºF)	40ºC (104ºF)	48ºC (118ºF)
f_1	60 Hz	65 Hz	100 Hz	110 Hz
f_2	130 Hz	130 Hz	-	190 Hz
f_3	170 Hz	160 Hz	190 Hz	210 Hz
ζ_1	0.02	0.02	0.02	0.02
ζ_2	0.02	0.02	-	0.02
ζ_3	0.02	0.02	0.02	0.02
k_1	-7e4	+2e4	-2e5	-2e5
k_2	-4e4	+4e4	0	-4e4
k_3	-4e5	+2e5	-2e5	-1e5

Table 4.4. Comparison of the Active Control Results for Different Temperatures [29]

Temperature	22ºC (72ºF)	28ºC (82ºF)	40ºC (104ºF)	48ºC (118ºF)
First Vibration Mode	47.5 Hz	56 Hz	93 Hz	107.5 Hz
% Reduction	**43%**	**54%**	**48%**	**32%**
Second Vibration Mode	119 Hz	116 Hz	-	188.5 Hz
% Reduction	**40%**	**39%**	**-**	**44%**
Third Vibration Mode	154 Hz	152 Hz	177 Hz	197 Hz
% Reduction	**34%**	**25%**	**37%**	**49%**

The results clearly indicate the potential of the active control system to work at wide temperature ranges. However, the varying temperature not only affects the actuator

and sensor system it also affects the structure to be controlled. This means that important characteristics like vibration frequencies and damping ratios of the structure might change significantly. The experiments under varying temperatures have shown this conclusively. Therefore, a control system designed to work for a wide range of temperatures must include online adaptive algorithms to fit the wide range of structure properties.

4.7 Summary

This chapter describes the test results obtained from the passive control system with shunted PZTs and the active control system. The specific tests setups used to obtain the results are also provided. In addition to the control system results, the results from the health monitoring system and the temperature variation tests are given. The results in this chapter clearly demonstrate the benefits of adding smart damping to structures.